KINETIC/FLUID MICRO-MACRO NUMERICAL SCHEME FOR A TWO COMPONENT PLASMA

ANAÏS CRESTETTO*, CHRISTIAN KLINGENBERG†, AND MARLIES PIRNER‡

Abstract. This work is devoted to the numerical simulation of the Vlasov-BGK equation for two species in the fluid limit using a particle method. Thus, we are interested in a plasma consisting of electrons and one species of ions without chemical reactions assuming that the number of particles of each species remains constant. We consider the kinetic two species model proposed by Klingenberg, Pirner and Puppo in [17], which separates the intra and interspecies collisions. Then, we propose a new model based on a micro-macro decomposition (see Bennoune, Lemou and Mieussens[3] and Crestetto, Crouseilles and Lemou[7]). The kinetic micro part is solved by a particle method, whereas the fluid macro part is discretized by a standard finite volume scheme. Main advantages of this approach are: (i) the noise inherent to the particle method is reduced compared to a standard (without micro-macro decomposition) particle method, (ii) the computational cost of the method is reduced in the fluid limit since a small number of particles is then sufficient.

Key words. Two species mixture, kinetic model, plasma flow, Vlasov equation, BGK equation, micro-macro decomposition, particles method.

AMS subject classifications. 65M75, 82C40, 82D10, 35B40.

1. Introduction.

We want to model a plasma consisting of two species, electrons and one species of ions. The kinetic description of a plasma is based on the Vlasov equation. In [7], Crestetto, Crouseilles and Lemou developed a numerical simulation of the Vlasov-BGK equation in the fluid limit using particles. They consider a Vlasov-BGK equation for the electrons and treat the ions as a background charge. In [7] a micro-macro decomposition is used as in [3] where asymptotic preserving schemes have been derived in the fluid limit. In [7], the approach in [3] is modified by using a particle approximation for the kinetic part, the fluid part being always discretized by standard finite volume schemes. Other approaches where kinetic description of one species is written in a micro-macro decomposition can be seen in [8, 9].

In this paper, we want to model both the electrons and the ions by a Vlasov-BGK equation instead of treating one only as a background charge. Such a two component kinetic description of the gas mixture has for example importance in a tokamak plasma. In regions nest to the wall of the tokamak, the plasma is close to a fluid, but the kinetic description is mandatory in the core plasma so that a hybrid fluid/kinetic description is adequate. For this, we want to use the approach in [7], since it has the following advantages: the presented scheme has a much less level of noise compared to the standard particle method and the computational cost of the micro-macro model is reduced in the fluid regime since a small number of particles is needed for the micro part.

From the modelling point of view, we want to describe this gas mixture using two distribution functions via the Vlasov equation with interaction terms on the right-hand side. For the interactions we use the BGK approach. BGK models give rise to efficient numerical computations, see for example [19, 13, 12, 3, 11, 4, 7]. In the literature one

*University of Nantes, 2 rue de la Houssinière, 44322 Nantes Cedex 3, France & INRIA Rennes - Bretagne Atlantique (anais.crestetto@univ-nantes.fr).

†University of Würzburg, Emil-Fischer-Str. 40, 97074 Würzburg, Germany (klingen@mathematik.uni-wuerzburg.de).

‡University of Würzburg, Emil-Fischer-Str. 40, 97074 Würzburg, Germany (marlies.pirner@mathematik.uni-wuerzburg.de).

can find two types of models for gas mixtures. Just like the Boltzmann equation for gas mixtures contains a sum of collision terms on the right-hand side, one type of model also has a sum collision terms in the relaxation operator. One example is the model of Klingenberg, Pirner and Puppo [17] which we will consider in this paper. It contains the often used models of Gross and Krook [14] and Hamel [15] as special cases. The other type of model contains only one collision term on the right-hand side. Example of this is the well-known model of Andries, Aoki and Perthame in [1]. In this paper we are interested in the first type of models, and use the model developed in [17]. In this type of model the two different types of interactions, interactions of a species with itself and interactions of a species with the other one, are kept separated. Therefore we can see how these different types of interactions influence the trend to equilibrium. From the physical point of view, we expect two different types of trends to equilibrium. For example, if the collision frequencies of the particles of each species with itself are larger compared to the collision frequencies related to interspecies collisions, we expect that we first observe that the relaxation of the two distribution functions to its own equilibrium distribution is faster compared to the relaxation towards a common velocity and a common temperature. This effect is clearly seen in the model presented in [17] since the two types of interactions are separated.

The outline of the paper is as follows: In section 2 we present the model for a plasma consisting of electrons and one species of ions and write it in dimensionless form. In section 3 we derive the micro-macro decomposition of the model presented in section 2. In section 4 we prove some convergence rates in the space-homogeneous case of the distribution function to a Maxwellian distribution and of the two velocities and temperatures to a common value which we will verify numerically later on. In section 5, we briefly present the numerical approximation, based on a particle method for the micro equation and a finite volume scheme for the macro one. In section 6, we present some numerical examples.First, we verify numerically the convergence rates obtained in section 4. Then, in the general case, we are interested in the evolution in time of the system. We consider different possibilities for the values of the collision frequencies. When the collision frequencies are very small we obtain the effect of Landau damping. When the collision frequencies are very large we observe relaxations towards Maxwellian distributions. Finally, if we vary the relationships between the different collision frequencies, we observe a corresponding variation in the speed of relaxation towards Maxwellians and the relaxation towards a common value of the mean velocities and temperatures. Finally, section 7 presents a brief conclusion.

2. The two-species model.

In this section we present in 1D the Vlasov-BGK model for a mixture of two species developed in [17] and mention its fundamental properties like the conservation properties. Then, we present its dimensionless form.

2.1. 1D Vlasov-BGK model for a mixture of two species.

We consider a plasma consisting of electrons denoted by the index e and one species of ions denoted by the index i. Thus, our kinetic model has two distribution functions $f_e(x, v, t) > 0$ and $f_i(x, v, t) > 0$ where $x \in [0, L_x], L_x > 0$, $v \in \mathbb{R}$ are the phase space variables and $t \geq 0$ the time.

Furthermore, for any $f_i, f_e : [0, L_x] \times \mathbb{R} \times \mathbb{R}_0^+ \to \mathbb{R}^+$ with $(1 + |v|^2)f_i$, $(1 + |v|^2)f_e \in L^1(\mathbb{R})$, we relate the distribution functions to macroscopic quantities by mean-values of f_k, $k = i, e$

$$\int f_k(v) \begin{pmatrix} 1 \\ v \\ m_k|v-u_k|^2 \end{pmatrix} dv =: \begin{pmatrix} n_k \\ n_k u_k \\ n_k T_k \end{pmatrix}, \quad k = i, e, \tag{1}$$

where m_k is the mass, n_k the number density, u_k the mean velocity and T_k the mean temperature of species k, $k = i, e$. Note that in this paper we shall write T_k instead of $k_B T_k$, where k_B is Boltzmann's constant.

We want to model the time evolution of the distribution functions by Vlasov-BGK equations. Each distribution function is determined by one Vlasov-BGK equation to describe its time evolution. The two equations are coupled through a term which describes the interaction of the two species. We consider binary interactions. So the particles of one species can interact with either themselves or with particles of the other species. In the model this is accounted for introducing two interaction terms in both equations. Here, we choose the collision terms as BGK operators, so that the model writes

$$\begin{aligned} &\partial_t f_i + v\partial_x f_i + \frac{F_i^L}{m_i}\,\partial_v f_i = \nu_{ii} n_i (M_i - f_i) + \nu_{ie} n_e (M_{ie} - f_i), \\ &\partial_t f_e + v\partial_x f_e + \frac{F_e^L}{m_e}\,\partial_v f_e = \nu_{ee} n_e (M_e - f_e) + \nu_{ei} n_i (M_{ei} - f_e), \end{aligned} \tag{2}$$

with the mean-field forces F_i^L and F_e^L specified later and the Maxwell distributions

$$\begin{aligned} M_k(x,v,t) &= \frac{n_k}{\sqrt{2\pi \frac{T_k}{m_k}}} \exp\Big(-\frac{|v-u_k|^2}{2\frac{T_k}{m_k}}\Big), \quad k = i, e, \\ M_{kj}(x,v,t) &= \frac{n_{kj}}{\sqrt{2\pi \frac{T_{kj}}{m_k}}} \exp\Big(-\frac{|v-u_{kj}|^2}{2\frac{T_{kj}}{m_k}}\Big), \quad k, j = i, e, k \neq j, \end{aligned} \tag{3}$$

where $\nu_{ii} n_i$ and $\nu_{ee} n_e$ are the collision frequencies of the particles of each species with itself, while $\nu_{ie} n_e$ and $\nu_{ei} n_i$ are related to interspecies collisions. To be flexible in choosing the relationship between the collision frequencies, we now assume the relationship

$$\begin{aligned} &\nu_{ie} = \varepsilon \nu_{ei}, && 0 < \varepsilon \leq 1, \\ &\nu_{ii} = \beta_i \nu_{ie}, \quad \nu_{ee} = \beta_e \nu_{ei} = \frac{\beta_e}{\varepsilon} \nu_{ie}, && \beta_i, \beta_e > 0. \end{aligned} \tag{4}$$

The restriction $\varepsilon \leq 1$ is without loss of generality. If $\varepsilon > 1$, exchange the notation i and e and choose $\frac{1}{\varepsilon}$. We assume that all collision frequencies are positive. In addition, we take into account an acceleration due to interactions using mean-field Lorentz forces F_i^L, F_e^L. We assume that the magnetic field is negligible compared to the electric field. Therefore the Lorentz forces are given by

$$F_i^L(x,t) = e\; E(x,t) \quad \text{and} \quad F_e^L(x,t) = -e\; E(x,t), \tag{5}$$

where e denotes the elementary charge. For simplicity, we assumed that the ions have the charge e. The electric field is given by the Maxwell equation

$$\partial_x E(x,t) = \rho(x,t), \tag{6}$$

where

$$\rho(x,t) = e\int_{-\infty}^{\infty}(f_i(x,v,t) - f_e(x,v,t))dv \tag{7}$$

describes the charge density.

The functions f_k and E are submitted to the following periodic condition

$$\begin{aligned} f_k(0,v,t) &= f_k(L_x,v,t), \quad \text{for every} \quad v \in \mathbb{R}, t \geq 0, \\ E(0,t) &= E(L_x,t), \quad \text{for every} \quad t \geq 0. \end{aligned}$$

In order to get a well-posed problem, a zero-mean electrostatic condition has to be added,

$$\int_0^{L_x} E(x,t)dx = 0, \quad \text{for every} \quad t \geq 0,$$

together with an initial condition

$$f_k(x,v,0) = f_k^0(x,v), \quad \text{for every} \quad x \in [0,L_x], v \in \mathbb{R}.$$

From the initial condition on f_k, we can compute an initial condition of the charge density ρ given by (7). From this we can compute the initial data of E using (6).

The Maxwell distributions M_i and M_e in (3) have the same moments as f_i and f_e respectively. With this choice, we guarantee the conservation of mass, momentum and energy in interactions of one species with itself (see section 2.2 in [17]). The remaining parameters $n_{ie}, n_{ei}, u_{ie}, u_{ei}, T_{ie}$ and T_{ei} will be determined using conservation of total momentum and energy, together with some symmetry considerations.

If we assume that

$$n_{ie} = n_i \quad \text{and} \quad n_{ei} = n_e, \tag{8}$$

$$u_{ie} = \delta u_i + (1-\delta)u_e, \quad \delta \in \mathbb{R}, \tag{9}$$

$$T_{ie} = \alpha T_i + (1-\alpha)T_e + \gamma|u_i - u_e|^2, \quad 0 \leq \alpha \leq 1, \gamma \geq 0, \tag{10}$$

we have conservation of the number of particles, of total momentum and total energy provided that

$$u_{ei} = u_e - \frac{m_i}{m_e}\varepsilon(1-\delta)(u_e - u_i), \quad \text{and} \tag{11}$$

$$\begin{aligned} T_{ei} = &\left[\varepsilon m_i(1-\delta)\left(\frac{m_i}{m_e}\varepsilon(\delta-1) + \delta + 1\right) - \varepsilon\gamma\right]|u_i - u_e|^2 \\ &+ \varepsilon(1-\alpha)T_i + (1-\varepsilon(1-\alpha))T_e, \end{aligned} \tag{12}$$

see theorem 2.1, theorem 2.2 and theorem 2.3 in [17].

In order to ensure the positivity of all temperatures, we need to impose restrictions on δ and γ given by

$$0 \leq \gamma \leq m_i(1-\delta)\left[(1 + \frac{m_i}{m_e}\varepsilon)\delta + 1 - \frac{m_i}{m_e}\varepsilon\right], \quad \text{and} \tag{13}$$

$$\frac{\frac{m_i}{m_e}\varepsilon - 1}{1 + \frac{m_i}{m_e}\varepsilon} \leq \delta \leq 1, \tag{14}$$

see theorem 2.5 in [17].

2.2. Dimensionless form. We want to write the BGK model presented in subsection 2.1 in dimensionless form. The principle of non-dimensionalization can also be found in chapter 2.2.1 in [20] for the Boltzmann equation and in [5] for macroscopic equations. First, we define dimensionless variables of the time $t \in \mathbb{R}_0^+$, the length $x \in [0, L_x]$, the velocity $v \in \mathbb{R}$, the distribution functions f_i, f_e, the number densities n_i, n_e, the mean velocities u_i, u_e, the temperatures T_i, T_e, the electric field E and of the collision frequency ν_{ie}. Then, dimensionless variables of the other collision frequencies $\nu_{ii}, \nu_{ee}, \nu_{ei}$ can be derived by using the relationships (4). We start with choosing typical scales denoted by a bar.

$$t' = t/\bar{t}, \quad x' = x/\bar{x}, \quad v' = v/\bar{v},$$

$$f_i'(x', v', t') = \frac{\bar{x}\bar{v}}{N_i} f_i(x, v, t), \quad f_e'(x', v', t') = \frac{\bar{x}\bar{v}}{N_e} f_e(x, v, t),$$

where N_i is the total number of ions and N_e the total number of electrons in the volume $\bar{x}$. We assume $N_i = N_e =: N$. This assumption is in accordance with the typical values in a plasma described in [5]. Further, we choose

$$n_i' = n_i/\bar{n}_i, \quad n_e' = n_e/\bar{n}_e, \quad \bar{n}_i = \bar{n}_e = \frac{N}{\bar{x}},$$

$$E' = E/\bar{E}$$

$$u_i' = u_i/\bar{u}_i, \quad u_e' = u_e/\bar{u}_e, \quad \bar{u}_e = \bar{u}_i = \bar{v},$$

$$T_i' = T_i/\bar{T}_i, \quad T_e' = T_e/\bar{T}_e, \quad \bar{T}_e = \bar{T}_i = m_i \bar{v}^2,$$

$$\nu_{ie}' = \nu_{ie}/\bar{\nu}_{ie}.$$

Now we want to write equations (2) in dimensionless variables. We start with the Maxwellians (3) and with (9)-(12). We replace the macroscopic quantities n_i, u_i and T_i in M_i by their dimensionless expressions and obtain

$$M_i = \frac{n_i' \bar{n}_i}{\sqrt{2\pi \frac{\bar{T}_i T_i'}{m_i}}} \exp\left(-\frac{|v'\bar{v} - u_i'\bar{u}_i|^2 m_i}{2 T_i' \bar{T}_i}\right). \tag{15}$$

If we assume that $\bar{v}^2 = |\bar{u}_i|^2 = \frac{\bar{T}_i}{m_i}$, we obtain

$$M_i = \frac{\bar{n}_i}{\bar{v}} \frac{n_i'}{\sqrt{2\pi T_i'}} \exp\left(-\frac{|v' - u_i'|^2}{2T_i'}\right) =: \frac{\bar{n}_i}{\bar{v}} M_i'. \tag{16}$$

The relationship on $\bar{u}_i$ and $\bar{T}_i$ used here is in accordance with the typical values in a plasma described in [5]. In the Maxwellian M_e we assume $\bar{T}_i = \bar{T}_e =: \bar{T}$ and obtain in the same way as for M_i

$$M_e = \frac{\bar{n}_e}{\bar{v}} \left(\frac{m_e}{m_i}\right)^{\frac{1}{2}} \frac{n_e'}{\sqrt{2\pi T_e'}} \exp\left(-\frac{|v' - u_e'|^2}{2T_e'} \frac{m_e}{m_i}\right) =: \frac{\bar{n}_e}{\bar{v}} M_e'. \tag{17}$$

Now, we consider the Maxwellian M_{ie} in (3), its velocity u_{ie} in (9) and its temperature T_{ie} in (10). Again we use $\bar{v} = \bar{u}_i = \bar{u}_e$ and $\bar{v}^2 = \frac{\bar{T}}{m_i} = \frac{\bar{T}_i}{m_i} = \frac{\bar{T}_e}{m_e}\frac{m_e}{m_i}$ and obtain

$$\begin{aligned} u_{ie} &= \delta u_i' \bar{u}_i + (1-\delta) u_e' \bar{u}_e = (\delta u_i' + (1-\delta) u_e')\bar{v} =: \bar{v} u_{ie}', \\ T_{ie} &= \alpha T_i' \bar{T}_i + (1-\alpha) T_e' \bar{T}_e + \gamma |\bar{v}|^2 |u_i' - u_e'|^2 \\ &= m_i |\bar{v}|^2 [\alpha T_i' + (1-\alpha) T_e' + \frac{\gamma}{m_i} |u_i' - u_e'|^2] =: |\bar{v}|^2 m_i T_{ie}', \\ M_{ie} &= \frac{n_i' \bar{n}_i}{\sqrt{2\pi \bar{v}^2 T_{ie}'}} \exp(-\frac{|v' - u_{ie}'|^2}{2T_{ie}'}) =: \frac{\bar{n}_i}{\bar{v}} M_{ie}'. \end{aligned} \tag{18}$$

With the same assumptions we obtain for u_{ei}, T_{ei} and M_{ei} in a similar way the expressions

$$\begin{aligned} u_{ei} &= [(1 - \frac{m_i}{m_e}\varepsilon(1-\delta))u_e' + \frac{m_i}{m_e}\varepsilon(1-\delta)u_i']\bar{v} =: u_{ei}'\bar{v}, \\ T_{ei} &= [(1-\varepsilon(1-\alpha))T_e' + \varepsilon(1-\alpha)T_i']\bar{T} \\ &\quad + (\varepsilon m_i (1-\delta)(\frac{m_i}{m_e}\varepsilon(\delta - 1) + \delta + 1) - \varepsilon\gamma)|u_i' - u_e'|^2 |\bar{v}|^2 \\ &= [(1-\varepsilon(1-\alpha))T_e' + \varepsilon(1-\alpha)T_i']|\bar{v}|^2 m_e \frac{m_i}{m_e} \\ &\quad + (\varepsilon m_i (1-\delta)(\frac{m_i}{m_e}\varepsilon(\delta - 1) + \delta + 1) - \varepsilon\gamma)|u_i' - u_e'|^2 |\bar{v}|^2 =: |\bar{v}|^2 m_e \frac{m_i}{m_e} T_{ei}', \\ M_{ei} &= \frac{\bar{n}_e}{\bar{v}} \frac{m_e}{m_i} \frac{n_e'}{\sqrt{2\pi T_{ei}'}} \exp(-\frac{|v' - u_{ei}'|^2}{2T_{ei}'}\frac{m_e}{m_i}) =: \frac{\bar{n}_e}{\bar{v}} M_{ei}'. \end{aligned}$$

Now we replace all quantities in (2) by their non-dimensionalized expressions. For the left-hand side of the equation for the ions we obtain

$$\begin{aligned} &\partial_t f_i + v \partial_x f_i + \frac{e}{m_i} E \partial_v f_i \\ &= \frac{1}{\bar{t}} \frac{N}{\bar{x}\bar{v}} \partial_{t'} f_i' + \frac{1}{\bar{x}} \frac{N}{\bar{x}\bar{v}} \bar{v} v' \partial_{x'} f_i' + \frac{N}{\bar{x}\bar{v}} \frac{1}{\bar{v}} \bar{E} \frac{e}{m_i} E' \partial_{v'} f_i' \end{aligned} \tag{19}$$

and for the right-hand side using that $\bar{n}_k = \frac{N}{\bar{x}}, k = i, e$, (4), (16) and (18), we get

$$\begin{aligned} &\nu_{ii} n_i (M_i - f_i) + \nu_{ie} n_e (M_{ie} - f_i) = \nu_{ie} \beta_i n_i (M_i - f_i) + \nu_{ie} n_e (M_{ie} - f_i) \\ &= \beta_i \bar{\nu}_{ie} \frac{N}{\bar{x}\bar{v}} \frac{N}{\bar{x}} \nu_{ie}' n_i' (M_i' - f_i') + \bar{\nu}_{ie} \frac{N}{\bar{x}\bar{v}} \frac{N}{\bar{x}} \nu_{ie}' n_e' (M_{ie}' - f_i'). \end{aligned} \tag{20}$$

Multiplying by $\frac{\bar{t}\bar{x}\bar{v}}{N}$ and dropping the primes in the variables leads to

$$\begin{aligned} &\partial_t f_i + \frac{\bar{t}\bar{v}}{\bar{x}} v \partial_x f_i + \bar{t}\frac{\bar{E}}{\bar{v}} \frac{e}{m_i} E \partial_v f_i \\ &= \beta_i \bar{\nu}_{ie} \bar{t} \frac{N}{\bar{x}} \nu_{ie} n_i (M_i - f_i) + \bar{\nu}_{ie} \bar{t} \frac{N}{\bar{x}} \nu_{ie} n_e (M_{ie} - f_i). \end{aligned}$$

In a similar way we obtain for electrons

$$\begin{aligned} &\partial_t f_e + \frac{\bar{t}\bar{v}}{\bar{x}} v \partial_x f_e - \bar{t}\frac{\bar{E}}{\bar{v}} \frac{e}{m_e} E \partial_v f_e \\ &= \frac{\beta_e}{\varepsilon} \bar{\nu}_{ie} \bar{t} \frac{N}{\bar{x}} \nu_{ie} n_e \left(M_e - f_e\right) + \frac{1}{\varepsilon} \bar{\nu}_{ie} \bar{t} \frac{N}{\bar{x}} \nu_{ie} n_i \left(M_{ei} - f_e\right), \end{aligned}$$

and the non-dimensionalized Maxwellians given by

$$
\begin{aligned}
M_i(x,v,t) &= \frac{n_i}{\sqrt{2\pi T_i}} \exp(-\frac{|v-u_i|^2}{2T_i}),\\
M_e(x,v,t) &= \frac{n_e}{\sqrt{2\pi T_e}} \left(\frac{m_e}{m_i}\right)^{\frac{1}{2}} \exp(-\frac{|v-u_e|^2}{2T_e}\frac{m_e}{m_i}),\\
M_{ie}(x,v,t) &= \frac{n_i}{\sqrt{2\pi T_{ie}}} \exp(-\frac{|v-u_{ie}|^2}{2T_{ie}}),\\
M_{ei}(x,v,t) &= \frac{n_e}{\sqrt{2\pi T_{ei}}} \left(\frac{m_e}{m_i}\right)^{\frac{1}{2}} \exp(-\frac{|v-u_{ei}|^2}{2T_{ei}}\frac{m_e}{m_i}),
\end{aligned} \tag{21}
$$

with the non-dimensionalized macroscopic quantities

$$u_{ie} = \delta u_i + (1-\delta)u_e, \tag{22}$$

$$T_{ie} = \alpha T_i + (1-\alpha)T_e + \frac{\gamma}{m_i}|u_i-u_e|^2, \tag{23}$$

$$u_{ei} = (1 - \frac{m_i}{m_e}\varepsilon(1-\delta))u_e + \frac{m_i}{m_e}\varepsilon(1-\delta)u_i, \tag{24}$$

$$
\begin{aligned}
T_{ei} &= [(1-\varepsilon(1-\alpha))T_e + \varepsilon(1-\alpha)T_i]\\
&\quad + (\varepsilon(1-\delta)(\frac{m_i}{m_e}\varepsilon(\delta-1)+\delta+1) - \varepsilon\frac{\gamma}{m_i})|u_i-u_e|^2.
\end{aligned} \tag{25}
$$

Defining dimensionless parameters

$$
\begin{aligned}
&A = \frac{\bar{t}\bar{v}}{\bar{x}}, \quad B_i = \bar{t}\frac{\bar{E}}{\bar{v}}\frac{e}{m_i}, \quad B_e = \bar{t}\frac{\bar{E}}{\bar{v}}\frac{e}{m_e},\\
&\frac{1}{\varepsilon_i} = \beta_i\bar{\nu}_{ie}\bar{t}\frac{N}{\bar{x}}, \quad \frac{1}{\tilde{\varepsilon}_i} = \bar{\nu}_{ie}\bar{t}\frac{N}{\bar{x}}, \quad \frac{1}{\varepsilon_e} = \frac{\beta_e}{\varepsilon}\bar{\nu}_{ie}\bar{t}\frac{N}{\bar{x}}, \quad \frac{1}{\tilde{\varepsilon}_e} = \frac{1}{\varepsilon}\bar{\nu}_{ie}\bar{t}\frac{N}{\bar{x}},
\end{aligned} \tag{26}
$$

we get

$$
\begin{aligned}
\partial_t f_i + A\partial_x v f_i + B_i E\partial_v f_i &= \frac{1}{\varepsilon_i}\nu_{ie}n_i(M_i - f_i) + \frac{1}{\tilde{\varepsilon}_i}\nu_{ie}n_e(M_{ie}-f_i),\\
\partial_t f_e + Av\partial_x f_e - B_e E\partial_v f_e &= \frac{1}{\varepsilon_e}\nu_{ie}n_e(M_e - f_e) + \frac{1}{\tilde{\varepsilon}_e}\nu_{ie}n_i(M_{ei}-f_e).
\end{aligned} \tag{27}
$$

In addition, we want to write the moments (1) in non-dimensionalized form. We can compute this in a similar way as for (2) and obtain after dropping the primes

$$
\begin{aligned}
&\int f_k dv = n_k, \quad \int v f_k dv = n_k u_k, \quad k = i, e,\\
&\frac{1}{n_i}\int |v-u_i|^2 f_i dv = T_i, \quad \frac{m_e}{m_i}\frac{1}{n_e}\int |v-u_e|^2 f_e dv = T_e.
\end{aligned} \tag{28}
$$

For the non-dimensionalized form of the Maxwell equation (6) we obtain after dropping the primes

$$\frac{\bar{E}}{eN}\partial_x E = \rho. \tag{29}$$

We assume that $\frac{\bar{E}}{eN} = 1$.

Remark 2.1. According to [2] there are the following relationships between the collision frequencies in the case of ions and electrons

$$\nu_{ee} = \nu_{ei} = \sqrt{\frac{m_i}{m_e}}\nu_{ii} = \frac{m_i}{m_e}\nu_{ie},$$

which means

$$\varepsilon = \frac{m_e}{m_i}, \quad \beta_e = 1, \quad \beta_i = \sqrt{\frac{m_i}{m_e}}.$$

3. Micro-Macro decomposition. In this section, we derive the micro-macro model equivalent to (27).

First, we take the dimensionless equations (27) and choose $A = B_e = \frac{m_i}{m_e} B_i = 1$. The choice $A = 1$ means $\bar{v} = \frac{\bar{x}}{\bar{t}}$. The choice $B_e = 1$ means that the reciprocal unit time scales are given by the cyclotron frequency of electrons in the $\frac{\bar{E}}{\bar{v}}-$ field, that is $\frac{1}{\bar{t}} = \frac{\bar{E}}{\bar{v}} \frac{e}{m_e}$.

Now, we propose to adapt the micro-macro decomposition presented in [3] and [7]. It is used for numerical methods to solve Boltzmann-like equations for mixtures to capture the right compressible Navier-Stokes dynamics at small Knudsen numbers. The idea is to write each distribution function as the sum of its own equilibrium part (verifying a fluid equation) and a rest (of kinetic-type). So, we decompose f_i and f_e as

$$f_i = M_i + g_{ii}, \quad f_e = M_e + g_{ee}. \tag{30}$$

Let us introduce $m(v) := \begin{pmatrix} 1 \\ v \\ |v|^2 \end{pmatrix}$ and the notation $\langle \cdot \rangle := \int \cdot \, dv$. Since f_i and M_i (resp. f_e and M_e) have the same moments: $\langle m(v) f_i \rangle = \langle m(v) M_i \rangle$ (resp. $\langle m(v) f_e \rangle = \langle m(v) M_e \rangle$), then the moments of g_{ii} (resp. g_{ee}) are zero:

$$\int m(v) g_{ii} dv = \int m(v) g_{ee} dv = 0. \tag{31}$$

With this decomposition we get from equation (27) of ions in dimensionless form

$$\begin{aligned} &\partial_t M_i + \partial_t g_{ii} + v\partial_x M_i + v\partial_x g_{ii} + \frac{m_e}{m_i} E \partial_v M_i + \frac{m_e}{m_i} E \partial_v g_{ii} \\ &\qquad = -\frac{1}{\varepsilon_i} \nu_{ie} n_i g_{ii} + \frac{1}{\tilde{\varepsilon}_i} \nu_{ie} n_e (M_{ie} - M_i - g_{ii}), \end{aligned} \tag{32}$$

and a similar equation for electrons.

Now we consider the Hilbert spaces $L^2_{M_k} = \{\phi \text{ such that } \phi M_k^{-\frac{1}{2}} \in L^2(\mathbb{R})\}$, $k = i, e$, with the weighted inner product $\langle \phi \psi M_k^{-1} \rangle$. We consider the subspace $\mathcal{N}_k$ =span $\{M_k, vM_k, |v|^2 M_k\}$, $k = i, e$. Let Π_{M_k} the orthogonal projection in $L^2_{M_k}$ on this subspace $\mathcal{N}_k$. This subspace has the orthonormal basis

$$\tilde{B}_k = \{\frac{1}{\sqrt{n_k}} M_k, \frac{(v-u_k)}{\sqrt{T_k m_i/m_k}} \frac{1}{\sqrt{n_k}} M_k, (\frac{|v-u_k|^2}{2T_k m_i/m_k} - \frac{1}{2}) \frac{1}{\sqrt{n_k}} M_k\} =: \{b_1^k, b_2^k, b_3^k\}.$$

Using this orthonormal basis of $\mathcal{N}_k$, one finds for any function $\phi \in L^2_{M_k}$ the following expression of $\Pi_{M_k}(\phi)$

$$\Pi_{M_k}(\phi) = \sum_{n=1}^{3}(\phi, b_n^k)b_n^k = \frac{1}{n_k}[\langle\phi\rangle + \frac{(v-u_k)\cdot\langle(v-u_k)\phi\rangle}{T_k m_i/m_k} + (\frac{|v-u_k|^2}{2T_k m_i/m_k} - \frac{1}{2})2\langle(\frac{|v-u_k|^2}{2T_k m_i/m_k} - \frac{1}{2})\phi\rangle]M_k. \tag{33}$$

This orthogonal projection $\Pi_{M_k}(\phi)$ has some elementary properties.

LEMMA 3.1 (Properties of Π_{M_k}). *We have, for $k = i, e$,*

$$(\mathbb{1} - \Pi_{M_k})(M_k) = (\mathbb{1} - \Pi_{M_k})(\partial_t M_k) = 0,$$
$$\Pi_{M_k}(g_{kk}) = \Pi_{M_k}(\partial_t g_{kk}) = (\mathbb{1} - \Pi_{M_k})(E\partial_v M_k) = 0,$$

and

$$\Pi_{M_i}(M_{ie}) = (1 + \frac{(v-u_i)(u_{ie}-u_i)}{T_i} + (\frac{|v-u_i|^2}{2T_i} - \frac{1}{2})(\frac{T_{ie}}{T_i} + \frac{|u_{ie}-u_i|^2}{T_i} - 1))M_i, \tag{34}$$

$$\Pi_{M_e}(M_{ei}) = (1 + \frac{(v-u_e)(u_{ei}-u_e)}{T_e m_i/m_e} + (\frac{|v-u_e|^2}{2T_e m_i/m_e} - \frac{1}{2})(\frac{T_{ei}}{T_e} + \frac{|u_{ei}-u_e|^2}{T_e m_i/m_e} - 1))M_e. \tag{35}$$

Proof. The proof of the first five equalities is analogue to the one species case and is given in [3]. Besides, using the explicit expression of Π_{M_k}, $k = i, e$, given by (33) we obtain (34)-(35) by direct computations. ∎

Now we apply the orthogonal projection $\mathbb{1} - \Pi_{M_i}$ to (32), use lemma 3.1 and obtain

$$\partial_t g_{ii} + (\mathbb{1} - \Pi_{M_i})(v\partial_x M_i) + (\mathbb{1} - \Pi_{M_i})(v\partial_x g_{ii}) + (\mathbb{1} - \Pi_{M_i})(\frac{m_e}{m_i}E\partial_v g_{ii}) = \frac{1}{\tilde{\varepsilon}_i}\nu_{ie}n_e(M_{ie} - \Pi_{M_i}(M_{ie})) - (\frac{1}{\varepsilon_i}\nu_{ie}n_i + \frac{1}{\tilde{\varepsilon}_i}\nu_{ie}n_e)g_{ii}.$$

Again with lemma 3.1 we replace $\Pi_{M_i}(M_{ie})$ by its explicit expression

$$\partial_t g_{ii} + (\mathbb{1} - \Pi_{M_i})(v\partial_x M_i) + (\mathbb{1} - \Pi_{M_i})(v\partial_x g_{ii}) + (\mathbb{1} - \Pi_{M_i})(\frac{m_e}{m_i}E\partial_v g_{ii}) = \frac{1}{\tilde{\varepsilon}_i}\nu_{ie}n_e(M_{ie} - (1 + \frac{(v-u_i)(u_{ie}-u_i)}{T_i} + (\frac{|v-u_i|^2}{2T_i} - \frac{1}{2})(\frac{T_{ie}}{T_i} + \frac{1}{T_i}|u_{ie}-u_i|^2 - 1))M_i) - (\frac{1}{\varepsilon_i}\nu_{ie}n_i + \frac{1}{\tilde{\varepsilon}_i}\nu_{ie}n_e)g_{ii}. \tag{36}$$

We take the moments of equation (32), use (31), and we get

$$\partial_t\langle m(v)M_i\rangle + \partial_x\langle m(v)vM_i\rangle + \partial_x\langle m(v)vg_{ii}\rangle + \langle m(v)\frac{m_e}{m_i}E\partial_v M_i\rangle + \langle m(v)\frac{m_e}{m_i}E\partial_v g_{ii}\rangle = \frac{1}{\tilde{\varepsilon}_i}\nu_{ie}n_e(\langle m(v)(M_{ie} - M_i)\rangle).$$

Using partial integration and the fact that the moments of g_{ii} are zero we get that the term $\langle mE\partial_v g_{ii}\rangle$ vanishes and so we have

$$\begin{aligned}\partial_t\langle m(v)M_i\rangle + \partial_x\langle m(v)vM_i\rangle + \partial_x\langle m(v)vg_{ii}\rangle + \langle m(v)\frac{m_e}{m_i}E\partial_v M_i\rangle \\ = \frac{1}{\tilde{\varepsilon}_i}\nu_{ie}n_e(\langle m(v)(M_{ie}-M_i)\rangle).\end{aligned} \tag{37}$$

In a similar way, we get an analogous coupled system for the electrons which is coupled with the system of the ions

$$\begin{aligned}\partial_t g_{ee} &+ (\mathbb{1}-\Pi_{M_e})(v\partial_x M_e) + (\mathbb{1}-\Pi_{M_e})(v\partial_x g_{ee}) - (\mathbb{1}-\Pi_{M_e})(E\partial_v g_{ee}) \\ &= \frac{1}{\tilde{\varepsilon}_e}\nu_{ie}n_i(M_{ei} - (1 + \frac{(v-u_e)(u_{ei}-u_e)}{T_e}\frac{m_e}{m_i} \\ &+ (\frac{|v-u_e|^2}{2T_e}\frac{m_e}{m_i} - \frac{1}{2})(\frac{T_{ei}}{T_e} + \frac{m_e}{m_iT_e}|u_{ei}-u_e|^2 - 1))M_e) \\ &- (\frac{1}{\varepsilon_e}\nu_{ie}n_e + \frac{1}{\tilde{\varepsilon}_e}\nu_{ie}n_i)g_{ee},\end{aligned} \tag{38}$$

$$\begin{aligned}\partial_t\langle mM_e\rangle + \partial_x\langle m(vM_e)\rangle + \partial_x\langle m(vg_{ee})\rangle - \langle mE\partial_v M_e\rangle \\ = \frac{1}{\tilde{\varepsilon}_e}\nu_{ie}n_i(\langle m(M_{ei}-M_e)\rangle).\end{aligned} \tag{39}$$

Now we have obtained a system of two microscopic equations (36), (38) and two macroscopic equations (37), (39). One can show that this system is an equivalent formulation of the BGK equations for ions and electrons. This is analogous to what is done in [7].

4. Space-homogeneous case without electric field.

In this section, we consider our model in the space-homogeneous case, without electric field, where we can prove an estimation of the decay rate of $||f_k(t) - M_k(t)||_{L^1(dv)}$, $|u_i(t)-u_e(t)|^2$ and $|T_i(t)-T_e(t)|^2$.

In the space-homogeneous case without electric field, the BGK model for mixtures (2) simplifies to

$$\begin{aligned}\partial_t f_i &= \frac{1}{\varepsilon_i}\nu_{ie}n_i(M_i - f_i) + \frac{1}{\tilde{\varepsilon}_i}\nu_{ie}n_e(M_{ie}-f_i), \\ \partial_t f_e &= \frac{1}{\varepsilon_e}\nu_{ie}n_e(M_e - f_e) + \frac{1}{\tilde{\varepsilon}_e}\nu_{ie}n_i(M_{ei}-f_e),\end{aligned} \tag{40}$$

and we let the reader adapt the micro-macro decomposition (36)-(37)-(38)-(39) to this case.

4.1. Decay rate for the BGK model for mixtures in the space-homogeneous case.

We denote by $H(f) = \int f\ln f dv$ the entropy of a function f and by $H(f|g) = \int f\ln\frac{f}{g}dv$ the relative entropy of f and g.

THEOREM 4.1. *In the space homogeneous case without electric field (40), we have the following decay rate of the distribution functions f_i and f_e*

$$||f_k - M_k||_{L^1(dv)} \leq 4e^{-\frac{1}{2}Ct}[H(f_i^0|M_i^0) + H(f_e^0|M_e^0)]^{\frac{1}{2}}, \quad k = i, e,$$

where C is a constant.

Proof. We consider the entropy production of species i defined by

$$D_i(f_i, f_e) = -\int \frac{1}{\varepsilon_i}\nu_{ie} n_i \ln f_i (M_i - f_i) dv - \int \frac{1}{\tilde{\varepsilon}_i}\nu_{ie} n_e \ln f_i (M_{ie} - f_i) dv.$$

Define $\phi : \mathbb{R}^+ \to \mathbb{R}, \phi(x) := x \ln x$. Then $\phi'(x) = \ln x + 1$, so we can deduce

$$D_i(f_i, f_e) = -\int \frac{1}{\varepsilon_i}\nu_{ie} n_i \phi'(f_i)(M_i - f_i) dv - \int \frac{1}{\tilde{\varepsilon}_i}\nu_{ie} n_e \phi'(f_i)(M_{ie} - f_i) dv,$$

since $\int (f_i - M_i) dv = \int (f_i - M_{ie}) dv = 0$. Moreover, we have $\phi''(x) = \frac{1}{x}$. So ϕ is convex and we obtain

$$\begin{aligned} D_i(f_i, f_e) &\geq \int \frac{1}{\varepsilon_i}\nu_{ie} n_i (\phi(f_i) - \phi(M_i)) dv + \int \frac{1}{\tilde{\varepsilon}_i}\nu_{ie} n_e (\phi(f_i) - \phi(M_{ie})) dv \\ &= \frac{1}{\varepsilon_i}\nu_{ie} n_i (H(f_i) - H(M_i)) + \frac{1}{\tilde{\varepsilon}_i}\nu_{ie} n_e (H(f_i) - H(M_{ie})). \end{aligned} \tag{41}$$

In the same way we get a similar expression for $D_e(f_e, f_i)$ just exchanging the indices i and e.

If we use that $\ln M_i$ is a linear combination of $1, v$ and $|v|^2$, we see that $\int (M_i - f_i) \ln M_i dv = 0$ since f_i and M_i have the same moments. With this we can compute that

$$H(f_i|M_i) = H(f_i) - H(M_i). \tag{42}$$

Moreover in the proof of theorem 2.7 in [17], we see that

$$\frac{1}{\tilde{\varepsilon}_i}\nu_{ie} n_e H(M_{ie}) + \frac{1}{\tilde{\varepsilon}_e}\nu_{ie} n_i H(M_{ei}) \leq \frac{1}{\tilde{\varepsilon}_i}\nu_{ie} n_e H(M_i) + \frac{1}{\tilde{\varepsilon}_e}\nu_{ie} n_i H(M_e). \tag{43}$$

With (42) and (43), we can deduce from (41) that

$$\begin{aligned} D_i(f_i, f_e) + D_e(f_e, f_i) \geq &\left(\frac{1}{\varepsilon_i}\nu_{ie} n_i + \frac{1}{\tilde{\varepsilon}_i}\nu_{ie} n_e\right) H(f_i|M_i) \\ &+ \left(\frac{1}{\varepsilon_e}\nu_{ie} n_e + \frac{1}{\tilde{\varepsilon}_e}\nu_{ie} n_i\right) H(f_e|M_e). \end{aligned} \tag{44}$$

We want to relate the time derivative of the relative entropies

$$\frac{d}{dt}(H(f_i|M_i) + H(f_e|M_e)) = \frac{d}{dt}\left[\int f_i \ln \frac{f_i}{M_i} dv + \int f_e \ln \frac{f_e}{M_e} dv\right].$$

to the entropy production in the following. First we use product rule and obtain

$$\begin{aligned} \frac{d}{dt}(H(f_i|M_i) + H(f_e|M_e)) = &\int \partial_t f_i \left(\ln \frac{f_i}{M_i} + 1\right) dv - \int \frac{f_i}{M_i} \partial_t M_i dv \\ &+ \int \partial_t f_e \left(\ln \frac{f_e}{M_e} + 1\right) dv - \int \frac{f_e}{M_e} \partial_t M_e dv. \end{aligned} \tag{45}$$

By using the explicit expression of $\partial_t M_i$, we can compute that $\int f_k \frac{\partial_t M_k}{M_k} dv = \partial_t n_k = 0, k = i, e$, since n_k is constant in the space-homogeneous case. In the first term on the right-hand side of (45), we insert $\partial_t f_i$ and $\partial_t f_e$ from equation (40) and obtain

$$\begin{aligned} \frac{d}{dt}(H(f_i|M_i) + H(f_e|M_e)) = &\int \left(\frac{1}{\varepsilon_i}\nu_{ie} n_i (M_i - f_i) + \frac{1}{\tilde{\varepsilon}_i}\nu_{ie} n_e (M_{ie} - f_i)\right) \ln f_i dv \\ &+ \int \left(\frac{1}{\varepsilon_e}\nu_{ie} n_e (M_e - f_e) + \frac{1}{\tilde{\varepsilon}_e}\nu_{ie} n_i (M_{ei} - f_e)\right) \ln f_e dv. \end{aligned}$$

Indeed, the terms with $\ln M_i$ (resp. $\ln M_e$) vanish since $\ln M_i$ (resp. $\ln M_e$) is a linear combination of $1, v$ and $|v|^2$ and our model satisfies the conservation of the number of particles, total momentum and total energy (see section 2.2 in [17]). All in all, we obtain

$$\frac{d}{dt}(H(f_i|M_i) + H(f_e|M_e)) = -(D_i(f_i, f_e) + D_e(f_e, f_i)). \tag{46}$$

Using (44) we obtain

$$\begin{aligned}
&\frac{d}{dt}(H(f_i|M_i) + H(f_e|M_e)) \\
&\quad \leq -[(\frac{1}{\varepsilon_i}\nu_{ie}n_i + \frac{1}{\tilde{\varepsilon}_i}\nu_{ie}n_e)H(f_i|M_i) + (\frac{1}{\varepsilon_e}\nu_{ie}n_e + \frac{1}{\tilde{\varepsilon}_e}\nu_{ie}n_i)H(f_e|M_e)] \\
&\quad \leq -\min\{\frac{1}{\varepsilon_i}\nu_{ie}n_i + \frac{1}{\tilde{\varepsilon}_i}\nu_{ie}n_e, \frac{1}{\varepsilon_e}\nu_{ie}n_e + \frac{1}{\tilde{\varepsilon}_e}\nu_{ie}n_i\}(H(f_i|M_i) + H(f_e|M_e)).
\end{aligned}$$

Define $C := \min\{\frac{1}{\varepsilon_i}\nu_{ie}n_i + \frac{1}{\tilde{\varepsilon}_i}\nu_{ie}n_e, \frac{1}{\varepsilon_e}\nu_{ie}n_e + \frac{1}{\tilde{\varepsilon}_e}\nu_{ie}n_i\}$, then we can deduce an exponential decay with Gronwall's identity

$$\begin{aligned}
H(f_k|M_k) &\leq H(f_i|M_i) + H(f_e|M_e) \\
&\leq e^{-Ct}[H(f_i^0|M_i^0) + H(f_e^0|M_e^0)], \quad k = i, e.
\end{aligned}$$

With the Ciszar-Kullback inequality (see proposition 1.1 in [18]) we get

$$\begin{aligned}
||f_k - M_k||_{L^1(dv)} &\leq ||f_i - M_i||_{L^1(dv)} + ||f_e - M_e||_{L^1(dv)} \\
&\leq 4e^{-\frac{1}{2}Ct}[H(f_i^0|M_i^0) + H(f_e^0|M_e^0)]^{\frac{1}{2}}.
\end{aligned}$$

∎

4.2. Decay rate for the velocities and temperatures in the space-homogeneous case. In this subsection we prove decay rates for the velocities u_i, u_e (resp. temperatures T_i, T_e) to a common values in the space-homogeneous case. We start with a decay of $|u_i - u_e|^2$.

THEOREM 4.2. *Suppose that ν_{ie} is constant in time. In the space-homogeneous case without electric field (40), we have the following decay rate of the velocities*

$$|u_i(t) - u_e(t)|^2 = e^{-2\nu_{ie}(1-\delta)\left(\frac{1}{\tilde{\varepsilon}_i}n_e + \frac{\varepsilon}{\tilde{\varepsilon}_e}\frac{m_i}{m_e}n_i\right)t}|u_i(0) - u_e(0)|^2.$$

Proof. If we multiply the equations (40) by v and integrate with respect to v, we obtain by using (22), (24) and (26)

$$\begin{aligned}
\partial_t(n_iu_i) &= \frac{1}{\tilde{\varepsilon}_i}\nu_{ie}n_en_i(u_{ie} - u_i) = \frac{1}{\tilde{\varepsilon}_i}\nu_{ie}n_en_i(1-\delta)(u_e - u_i), \\
\partial_t(n_eu_e) &= \frac{1}{\tilde{\varepsilon}_e}\nu_{ie}n_en_i(u_{ei} - u_e) = \frac{1}{\tilde{\varepsilon}_e}\nu_{ie}n_en_i\frac{m_i}{m_e}\varepsilon(1-\delta)(u_i - u_e).
\end{aligned}$$

Since in the space-homogeneous case the densities n_i and n_e are constant, we actually have

$$\partial_tu_i = \frac{1}{\tilde{\varepsilon}_i}\nu_{ie}n_e(1-\delta)(u_e - u_i), \quad \partial_tu_e = \frac{1}{\tilde{\varepsilon}_e}\nu_{ie}n_i\frac{m_i}{m_e}\varepsilon(1-\delta)(u_i - u_e).$$

With this we get

$$
\begin{aligned}
\frac{1}{2}\frac{d}{dt}|u_i-u_e|^2 &= (u_i-u_e)\partial_t(u_i-u_e)\\
&= (u_i-u_e)\nu_{ie}(1-\delta)\left(\frac{1}{\tilde{\varepsilon}_i}n_e+\frac{\varepsilon}{\tilde{\varepsilon}_e}\frac{m_i}{m_e}n_i\right)(u_e-u_i)\\
&= -\nu_{ie}(1-\delta)\left(\frac{1}{\tilde{\varepsilon}_i}n_e+\frac{\varepsilon}{\tilde{\varepsilon}_e}\frac{m_i}{m_e}n_i\right)|u_i-u_e|^2.
\end{aligned}
$$

From this, we deduce

$$
|u_i(t)-u_e(t)|^2 = e^{-2\nu_{ie}(1-\delta)\left(\frac{1}{\tilde{\varepsilon}_i}n_e+\frac{\varepsilon}{\tilde{\varepsilon}_e}\frac{m_i}{m_e}n_i\right)t}|u_i(0)-u_e(0)|^2. \qquad \square
$$

We continue with a decay rate of $|T_i(t)-T_e(t)|$.

THEOREM 4.3. *Suppose ν_{ie} is constant in time. In the space-homogeneous case without electric field (40), we have the following decay rate of the temperatures*

$$
|T_i(t)-T_e(t)|^2 \le e^{-C_1 t}\left[|T_i(0)-T_e(0)| + \frac{|C_2|}{C_1-C_3}(e^{(C_1-C_3)t}-1)|u_i(0)-u_e(0)|^2\right],
$$

where the constants are defined by

$$
\begin{aligned}
C_1 &= (1-\alpha)\nu_{ie}\left(\frac{1}{\tilde{\varepsilon}_i}n_e+\frac{\varepsilon}{\tilde{\varepsilon}_e}n_i\right),\\
C_2 &= \nu_{ie}\left(\frac{1}{\tilde{\varepsilon}_i}n_e\left((1-\delta)^2+\frac{\gamma}{m_i}\right)-\frac{\varepsilon}{\tilde{\varepsilon}_e}n_i\left(1-\delta^2-\frac{\gamma}{m_i}\right)\right),\\
C_3 &= 2\nu_{ie}(1-\delta)\left(\frac{1}{\tilde{\varepsilon}_i}n_e+\frac{\varepsilon}{\tilde{\varepsilon}_e}\frac{m_i}{m_e}n_i\right).
\end{aligned}
$$

Proof. If we multiply the first equation of (40) by $\frac{1}{n_i}|v-u_i|^2$ and integrate with respect to v, we obtain

$$
\int \frac{1}{n_i}|v-u_i|^2\partial_t f_i dv = \frac{1}{\tilde{\varepsilon}_i}\nu_{ie}n_e\frac{1}{n_i}\int |v-u_i|^2(M_{ie}-f_i)dv. \tag{47}
$$

Indeed, the first relaxation term vanishes since M_i and f_i have the same temperature. We simplify the left-hand side of (47) to

$$
\begin{aligned}
\int \frac{1}{n_i}|v-u_i|^2\partial_t f_i dv &= \int \frac{1}{n_i}\partial_t(|v-u_i|^2 f_i)dv + 2\int \frac{1}{n_i}f_i(v-u_i)\cdot\partial_t u_i dv\\
&= \partial_t(T_i)+0,
\end{aligned}
$$

since the density n_i is constant. The right-hand side of (47) simplifies to

$$
\begin{aligned}
\frac{1}{\tilde{\varepsilon}_i}\nu_{ie}n_e\frac{1}{n_i}\int |v-u_i|^2(M_{ie}-f_i)dv &= \frac{1}{\tilde{\varepsilon}_i}\nu_{ie}n_e(T_{ie}+|u_{ie}-u_i|^2-T_i)\\
&= \frac{1}{\tilde{\varepsilon}_i}\nu_{ie}n_e\left((1-\alpha)(T_e-T_i)+\left((1-\delta)^2+\frac{\gamma}{m_i}\right)|u_e-u_i|^2\right).
\end{aligned}
$$

For the second species we multiply the second equation of (40) by $\frac{m_e}{m_i}\frac{1}{n_e}|v-u_e|^2$. For the left-hand side, we obtain by using (28)

$$
\int \frac{m_e}{m_i}\frac{1}{n_e}|v-u_e|^2\partial_t f_e dv = \partial_t T_e,
$$

and for the right-hand side using (24), (25) and (26)

$$\frac{1}{\tilde{\varepsilon}_e}\nu_{ie}n_i\frac{m_e}{m_i}\frac{1}{n_e}\int|v-u_e|^2(M_{ei}-f_e)dv=\frac{1}{\tilde{\varepsilon}_e}\nu_{ie}n_i(T_{ei}+\frac{m_e}{m_i}|u_{ei}-u_e|^2-T_e)$$
$$=\frac{1}{\tilde{\varepsilon}_e}\nu_{ie}n_i\left[\varepsilon(1-\alpha)(T_i-T_e)\right.$$
$$\left.+\left(\varepsilon(1-\delta)\left(\frac{m_i}{m_e}\varepsilon(\delta-1)+\delta+1\right)-\varepsilon\frac{\gamma}{m_i}+\varepsilon^2(1-\delta)^2\frac{m_i}{m_e}\right)|u_i-u_e|^2\right]$$
$$=\frac{1}{\tilde{\varepsilon}_e}\nu_{ie}n_i\left(\varepsilon(1-\alpha)(T_i-T_e)+\varepsilon(1-\delta^2-\frac{\gamma}{m_i})|u_i-u_e|^2\right).$$

So, we obtain

$$\partial_t T_i=\frac{1}{\tilde{\varepsilon}_i}\nu_{ie}n_e\left((1-\alpha)(T_e-T_i)+\left((1-\delta)^2+\frac{\gamma}{m_i}\right)|u_e-u_i|^2\right),$$
$$\partial_t T_e=\frac{1}{\tilde{\varepsilon}_e}\nu_{ie}n_i\left(\varepsilon(1-\alpha)(T_i-T_e)+\varepsilon\left(1-\delta^2-\frac{\gamma}{m_i}\right)|u_i-u_e|^2\right).$$

We deduce

$$\partial_t(T_i-T_e)=-(1-\alpha)\nu_{ie}\left(\frac{1}{\tilde{\varepsilon}_i}n_e+\frac{\varepsilon}{\tilde{\varepsilon}_e}n_i\right)(T_i-T_e)$$
$$+\nu_{ie}\left(\frac{1}{\tilde{\varepsilon}_i}n_e\left((1-\delta)^2+\frac{\gamma}{m_i}\right)-\frac{\varepsilon}{\tilde{\varepsilon}_e}n_i\left(1-\delta^2-\frac{\gamma}{m_i}\right)\right)|u_i-u_e|^2,$$

or with the constants defined in this theorem 4.3

$$\partial_t(T_i-T_e)=-C_1(T_i-T_e)+C_2|u_i-u_e|^2.$$

Duhamel's formula gives

$$T_i(t)-T_e(t)=e^{-C_1t}(T_i(0)-T_e(0))+C_2e^{-C_1t}\int_0^t e^{C_1s}|u_i(s)-u_e(s)|^2ds.$$

So we have the following inequality

$$|T_i(t)-T_e(t)|\le e^{-C_1t}|T_i(0)-T_e(0)|+|C_2|e^{-C_1t}\int_0^t e^{C_1s}|u_i(s)-u_e(s)|^2ds,$$

and by using theorem 4.2, we have

$$|T_i(t)-T_e(t)|\le e^{-C_1t}|T_i(0)-T_e(0)|+|C_2|e^{-C_1t}\int_0^t e^{C_1s}e^{-C_3s}ds|u_i(0)-u_e(0)|^2,$$
$$|T_i(t)-T_e(t)|\le e^{-C_1t}\left(|T_i(0)-T_e(0)|+\frac{|C_2|}{C_1-C_3}(e^{(C_1-C_3)t}-1)|u_i(0)-u_e(0)|^2\right) \square$$

5. Numerical approximation. This section is devoted to the numerical approximation of the two-species micro-macro system (36)-(37)-(38)-(39). Following the idea of [7], we propose to use a particle method to discretize both microscopic equations (36)-(38), in order to reduce the cost of the method when approaching the Maxwellian equilibrium. Macroscopic equations (37)-(39) are solved by a classical Finite Volume method.

In this paper, we only present the big steps of the method and refer to [7] for the details.

For the microscopic parts, we use a Particle-In-Cell method (see for example [6]): we approach g_{ii} (resp. g_{ee}) by a set of N_{p_i} (resp. N_{p_e}) particles, with position $x_{i_k}(t)$ (resp. $x_{e_k}(t)$), velocity $v_{i_k}(t)$ (resp. $v_{e_k}(t)$) and weight $\omega_{i_k}(t)$ (resp. $\omega_{e_k}(t)$), $k = 1,\dots,N_{p_i}$ (resp. $k = 1,\dots,N_{p_e}$). Then we assume that the microscopic distribution functions have the following expression:

$$g_{ii}(x,v,t) = \sum_{k=1}^{N_{p_i}} \omega_{i_k}(t)\delta(x - x_{i_k}(t))\delta(v - v_{i_k}(t)),$$

$$g_{ee}(x,v,t) = \sum_{k=1}^{N_{p_e}} \omega_{e_k}(t)\delta(x - x_{e_k}(t))\delta(v - v_{e_k}(t)),$$

with δ the Dirac mass. Moreover, we have the following relations:

$$\omega_{i_k}(t) = g_{ii}(x_{i_k}(t), v_{i_k}(t), t)\frac{L_x L_v}{N_{p_i}},\ k = 1,\dots,N_{p_i},$$

$$\omega_{e_k}(t) = g_{ee}(x_{e_k}(t), v_{e_k}(t), t)\frac{L_x L_v}{N_{p_e}},\ k = 1,\dots,N_{p_e},$$

where $L_x \in \mathbb{R}$ (resp. $L_v \in \mathbb{R}$) denotes the length of the domain in the space (resp. velocity) direction.

The method consists now in splitting the transport and the source parts of (36) (resp.(38)). Let us consider (36), the steps being the same for (38). The transport part

$$\partial_t g_{ii} + v\partial_x g_{ii} + E\partial_v g_{ii} = 0, \tag{48}$$

is solved by pushing the particles, that is evolving the positions and velocities thanks to the equations of motion:

$$\mathrm{d}_t x_{i_k}(t) = v_{i_k}(t), \quad \mathrm{d}_t v_{i_k}(t) = E(x_{i_k}(t), t), \quad \forall\ k = 1,\dots,N_{p_i}.$$

The source part

(49)
$$\begin{aligned}\partial_t g_{ii} =& -(\mathbb{1} - \Pi_{M_i})(v\partial_x M_i) + \Pi_{M_i}(v\partial_x g_{ii}) + \Pi_{M_i}(E\partial_v g_{ii})\\ &+ \frac{1}{\tilde{\varepsilon}_i}\nu_{ie} n_e(M_{ie} - (1 + \frac{(v-u_i)(u_{ie}-u_i)}{T_i}\\ &+ (\frac{|v-u_i|^2}{2T_i} - \frac{1}{2})(\frac{T_{ie}}{T_i} + \frac{1}{T_i}|u_{ie}-u_i|^2 - 1))M_i) - (\frac{1}{\varepsilon_i}\nu_{ie} n_i + \frac{1}{\tilde{\varepsilon}_i}\nu_{ie} n_e)g_{ii},\end{aligned}$$

is solved by evolving the weights. Let us denote by $S(x,v,t)$ the right-hand side such that $\partial_t g_{ii} = S(x,v,t)$. We compute the weight corresponding to S using the relation $s_{i_k}(t) = S(x_{i_k}(t), v_{i_k}(t), t)\frac{L_x L_v}{N_{p_i}},\ k = 1,\dots,N_{p_i}$ and then solve

$$\mathrm{d}_t \omega_{i_k}(t) = s_{i_k}(t).$$

The strategy is the same as in paragraph 4.1.2 of [7], where only one species is considered (and so there is no coupling terms). The supplementary terms coming from the coupling of both species are treated in the source part as the other source terms. They do not add particular difficulty.

A projection step, similar to the matching procedure of [10], ensures the preservation of the micro-macro structure (30) and in particular the property (31) on the moments of g_{ii} (resp. g_{ee}). Details are given in subsection 4.2 of [7].

Finally, macroscopic equations (37)-(39) are discretized on a grid in space and solved by a classical Finite Volume method. For the one species case, this is detailed in subsection 4.3 of [7]. The electric field is discretized on the same grid and computed at each time step by solving the Maxwell equation (6) with Finite Differences or Fast Fourier Transform.

6. Numerical results. We present in this section some numerical experiments obtained by the numerical approximation presented in section 5. A first series of tests aims at verifying numerically the decay rates of velocities and temperatures proved in subsection 4.2 in the space-homogeneous case without electric field. In a second series of tests, we are interested in the evolution in time of distribution functions, velocities, temperatures and electric energy in the general case. In particular, we want to see the influence of the collision frequencies.

In all this section, we consider the phase-space domain $(x, v) \in [0, 4\pi] \times [-10, 10]$ (assuming that physical particles of velocity v such that $|v| > 10$ can be negligible), so that $L_x = 4\pi$ and $L_v = 20$.

6.1. Decay rates in the space-homogeneous case. We first propose to validate our model in the space-homogeneous case, without electric field, where we have an estimation of the decay rate of $|u_i(t) - u_e(t)|^2$ and of $|T_i(t) - T_e(t)|$ (see section 4). Note that as in section 4, we simplify the notations: $u_i(x, t) = u_i(t)$, $u_e(x, t) = u_e(t)$, $T_i(x, t) = T_i(t)$, $T_e(x, t) = T_e(t)$.

We apply a simplified version of the numerical approximation presented in section 5, adapted to the space-homogeneous system (40) in its micro-macro form. For different initial conditions, we plot the evolution in time of $|u_i(t) - u_e(t)|^2$ (resp. $|T_i(t) - T_e(t)|$) and compare it to the estimates given in theorem 4.2 (resp. theorem 4.3). For all of these tests, we take $N_{p_i} = N_{p_e} = 10^4$ and $\Delta t = 10^{-4}$.

The first initial condition we consider corresponds to two Maxwellian functions:

$$f_i(v, t = 0) = \frac{n_i}{\sqrt{2\pi T_i(t = 0)}} \exp\left(-\frac{|v - u_i(t = 0)|^2}{2T_i(t = 0)}\right), \tag{50}$$

$$f_e(v, t = 0) = \frac{n_e}{\sqrt{2\pi T_e(t = 0)\frac{m_i}{m_e}}} \exp\left(-\frac{|v - u_e(t = 0)|^2}{2T_e(t = 0)}\frac{m_e}{m_i}\right), \tag{51}$$

with the following parameters: $n_i = 1$, $u_i(t = 0) = 0.5$, $T_i(t = 0) = 1$, $m_i = 1$, $n_e = 1.2$, $u_e(t = 0) = 0.1$, $T_e(t = 0) = 0.1$, $m_e = 1.5$, chosen as in subsection 5.1 of [16]. Results for $\varepsilon_i = \varepsilon_e = \tilde{\varepsilon}_i = \tilde{\varepsilon}_e = 0.05$ are given in figure 1 and results for $\varepsilon_i = \varepsilon_e = \tilde{\varepsilon}_i = \tilde{\varepsilon}_e = 0.01$ are given in figure 2. In these two cases, we plot $|u_i(t) - u_e(t)|$ too. As in [16], we remark that when the Knudsen numbers are smaller, the velocities, as well as the temperatures, converge faster to the equilibrium.

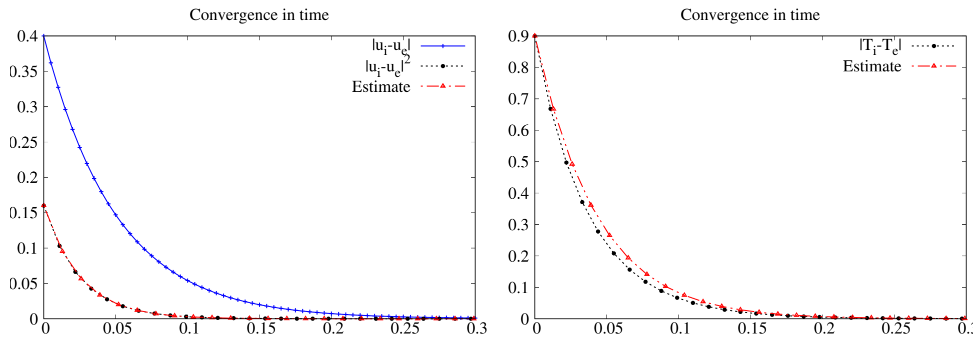

FIG. 1. *Space-homogeneous case. Maxwellians initial conditions. Evolution in time of* $|u_i(t) - u_e(t)|$, $|u_i(t) - u_e(t)|^2$ *(left) and* $|T_i(t) - T_e(t)|$ *(right). Comparison to the estimated decay rates. Knudsen numbers:* $\varepsilon_i = \varepsilon_e = \tilde{\varepsilon}_i = \tilde{\varepsilon}_e = 0.05$.

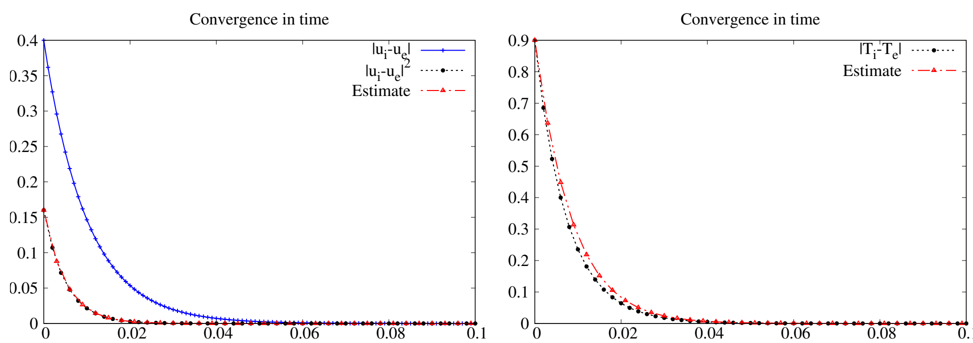

FIG. 2. *Space-homogeneous case. Maxwellians initial conditions. Evolution in time of* $|u_i(t) - u_e(t)|$, $|u_i(t) - u_e(t)|^2$ *(left) and* $|T_i(t) - T_e(t)|$ *(right). Comparison to the estimated decay rates. Knudsen numbers:* $\varepsilon_i = \varepsilon_e = \tilde{\varepsilon}_i = \tilde{\varepsilon}_e = 0.01$.

We propose now to consider $T_i(t = 0) = 0.08$ (other parameters are unchanged) and to study two other sets of Knudsen numbers. Results for $\varepsilon_i = \varepsilon_e = \tilde{\varepsilon}_i = \tilde{\varepsilon}_e = 1$ are given in figure 3 and results for $\varepsilon_i = \varepsilon_e = \tilde{\varepsilon}_i = 1$, $\tilde{\varepsilon}_e = 0.05$ are given in figure 4.

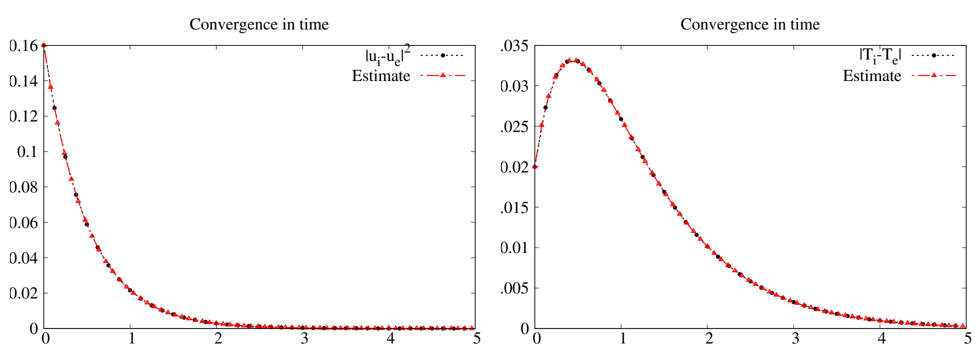

FIG. 3. *Space-homogeneous case. Maxwellians initial conditions. Evolution in time of* $|u_i(t) - u_e(t)|^2$ *(left) and* $|T_i(t) - T_e(t)|$ *(right). Comparison to the estimated decay rates. Knudsen numbers:* $\varepsilon_i = \varepsilon_e = \tilde{\varepsilon}_i = \tilde{\varepsilon}_e = 1$.

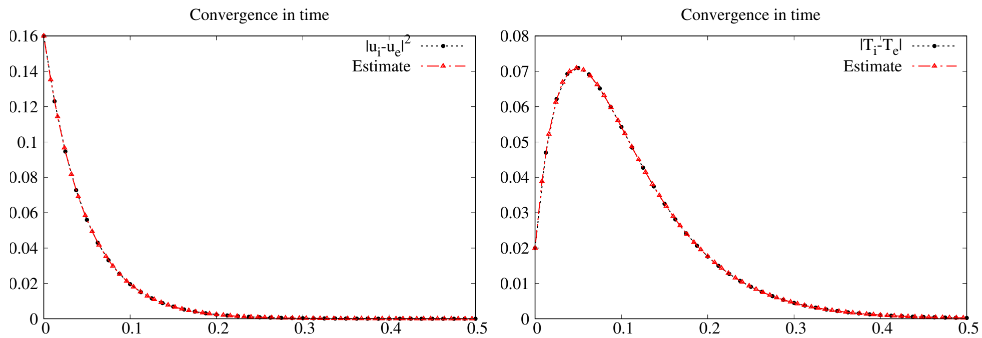

FIG. 4. *Space-homogeneous case. Maxwellians initial conditions. Evolution in time of* $|u_i(t) - u_e(t)|^2$ *(left) and* $|T_i(t)-T_e(t)|$ *(right). Comparison to the estimated decay rates. Knudsen numbers:* $\varepsilon_i = \varepsilon_e = \tilde{\varepsilon}_i = 1$, $\tilde{\varepsilon}_e = 0.05$.

We propose then to study the convergence for an other initial condition, considering

$$f_i(v, t = 0) = \frac{v^4}{3\sqrt{2\pi}} \exp\left(-\frac{|v|^2}{2}\right), \tag{52}$$

$$f_e(v, t = 0) = \frac{n_e}{\sqrt{2\pi T_e(t = 0) m_i/m_e}} \exp\left(-\frac{|v - u_e(t = 0)|^2}{2T_e(t = 0)} \frac{m_e}{m_i}\right), \tag{53}$$

with the following parameters: $n_e = 1.2$, $u_e(t = 0) = 0.1$, $T_e(t = 0) = 0.1$, $m_e = 1.5$. Here, the initial distribution of ions is not a Maxwellian, and then $g_{ii}(v, t = 0) \neq 0$. The estimates of theorems 4.2 and 4.3 are still verified, as we can see on figure 5 for $\varepsilon_i = \varepsilon_e = \tilde{\varepsilon}_i = \tilde{\varepsilon}_e = 1$. By taking now $T_e(t = 0) = 5$ (the other parameters being unchanged), we obtain results presented on figure 6.

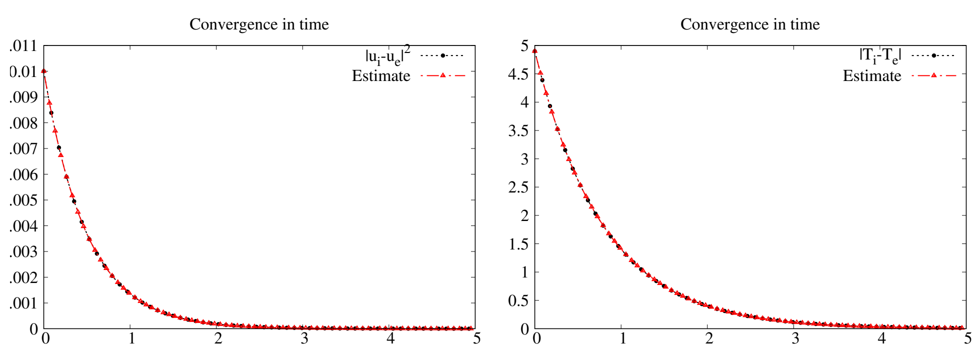

FIG. 5. *Space-homogeneous case. Mixed initial conditions. Evolution in time of* $|u_i(t) - u_e(t)|^2$ *(left) and* $|T_i(t) - T_e(t)|$ *(right). Comparison to the estimated decay rates. Knudsen numbers:* $\varepsilon_i = \varepsilon_e = \tilde{\varepsilon}_i = \tilde{\varepsilon}_e = 1$.

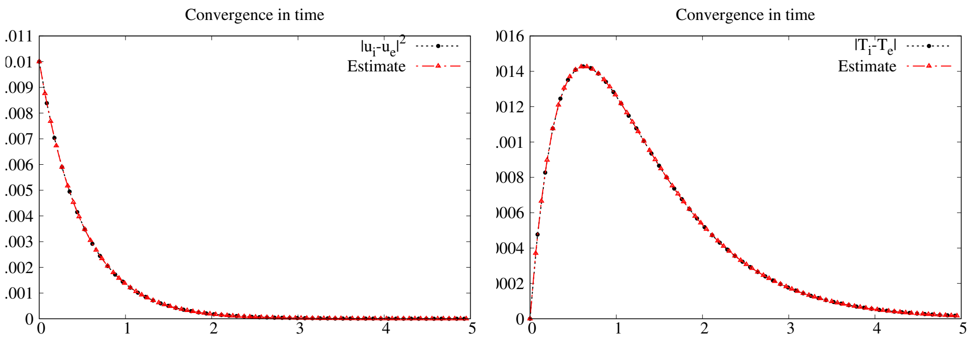

FIG. 6. *Space-homogeneous case. Mixed initial conditions. Evolution in time of* $|u_i(t) - u_e(t)|^2$ *(left) and* $|T_i(t) - T_e(t)|$ *(right). Comparison to the estimated decay rates. Knudsen numbers:* $\varepsilon_i = \varepsilon_e = \tilde{\varepsilon}_i = \tilde{\varepsilon}_e = 1$.

6.2. Relaxation towards a global equilibrium. We present here numerical results in the general (non homogeneous) case. We consider micro-macro equations (36)-(37)-(38)-(39) and discretize them as explained in section 5.

We are interested in the evolution in time of the distribution functions f_i, f_e and other quantities such as the electric energy $\mathcal{E}(t) := \sqrt{\int E(x,t)^2 dx}$, the difference of ions and electrons velocities (resp. temperatures) in uniform norm $||u_i(x,t) - u_e(x,t)||_\infty$ (resp. $||T_i(x,t) - T_e(x,t)||_\infty$). Different values of ε_i, ε_e, $\tilde{\varepsilon_i}$ and $\tilde{\varepsilon_e}$ are considered in order to see the influence of the intra and interspecies collision frequencies.

In the following tests, electrons and ions are initialized following

$$f_e(x, v, t = 0) = (1 + \alpha \cos(x/2)) \frac{v^4}{3\sqrt{2\pi}} \exp\left(-\frac{|v|^2}{2}\right), \tag{54}$$

$$f_i(x, v, t = 0) = \frac{1}{\sqrt{2\pi}} \exp\left(-\frac{|v - 1/2|^2}{2}\right). \tag{55}$$

So, for $\alpha \neq 0$, electrons have initially a space dependent distribution. From the computation of $\langle m(v) f_e \rangle$, we obtain $n_e(x, 0) = 1 + \alpha \cos(kx)$, $u_e(x, 0) = 0$ and $T_e(x, 0) = 5\,(1 + \alpha \cos(kx))$. Ions have initially a Maxwellian distribution with $n_i(x, 0) = 1$, $u_i(x, 0) = 1/2$ and $T_i(x, 0) = 1$. Here, we have taken $m_e = m_i = 1$.

For $\alpha = 0.1$, we illustrate the initial distribution functions on figure 7, $f_e(x, v, t = 0)$ is presented on the left, $f_i(x, v, t = 0)$ on the middle and a side view of them on the right.

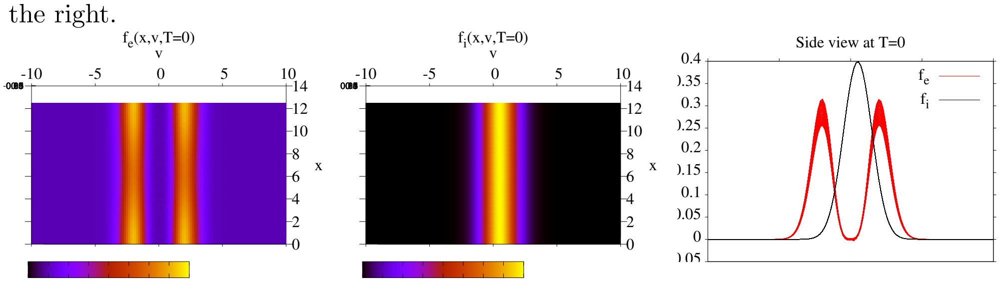

FIG. 7. *General case. Initial distribution functions for* $\alpha = 0.1$*:* $f_e(x, v, t = 0)$ *in phase-space (left),* $f_i(x, v, t = 0)$ *in phase-space (middle), side view of* $f_e(x, v, t = 0)$ *and* $f_i(x, v, t = 0)$ *(right).*

First, we propose two testcases with the following parameters: $\alpha = 0.1$, $N_{p_e} = N_{p_i} = 5 \cdot 10^5$, $N_x = 128$ and $\Delta t = 10^{-2}$. The first one consists in the kinetic regime

$\varepsilon_i = \varepsilon_e = \tilde{\varepsilon_i} = \tilde{\varepsilon_e} = 1000$, collision frequencies are small and particles do not interact a lot with each other. Distribution functions are plotted at time $T = 6$ on figure 8 and at time $T = 60$ on figure 9.

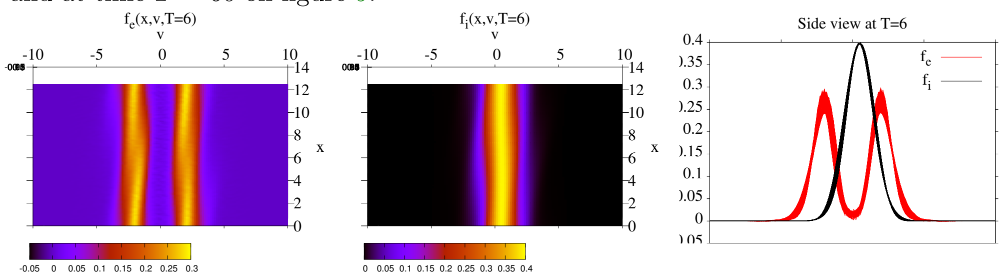

FIG. 8. *General case, $\alpha = 0.1$, $\varepsilon_i = \varepsilon_e = \tilde{\varepsilon_i} = \tilde{\varepsilon_e} = 1000$. Distribution functions at time $T = 6$: $f_e(x, v, T)$ in phase-space (left), $f_i(x, v, T)$ in phase-space (middle), side view of $f_e(x, v, T)$ and $f_i(x, v, T)$ (right).*

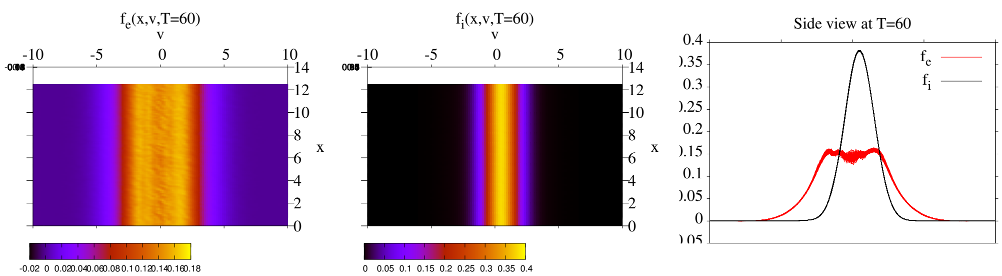

FIG. 9. *General case, $\alpha = 0.1$, $\varepsilon_i = \varepsilon_e = \tilde{\varepsilon_i} = \tilde{\varepsilon_e} = 1000$. Distribution functions at time $T = 60$: $f_e(x, v, T)$ in phase-space (left), $f_i(x, v, T)$ in phase-space (middle), side view of $f_e(x, v, T)$ and $f_i(x, v, T)$ (right).*

For these values of collision frequencies, the convergence of f_e towards its equilibrium M_e is slow. Moreover, even at time $T = 60$, the convergence towards a global equilibrium $f_e = M_e = M_i = f_i$ can not be seen. To see the difference on macroscopic quantities, we present on figure 10 (left) the evolution in time of $||u_i(x, t) - u_e(x, t)||_\infty$ and $||T_i(x, t) - T_e(x, t)||_\infty$. Moreover, we present on figure 10 (right) the evolution in time of the electric energy $\mathcal{E}(t)$.

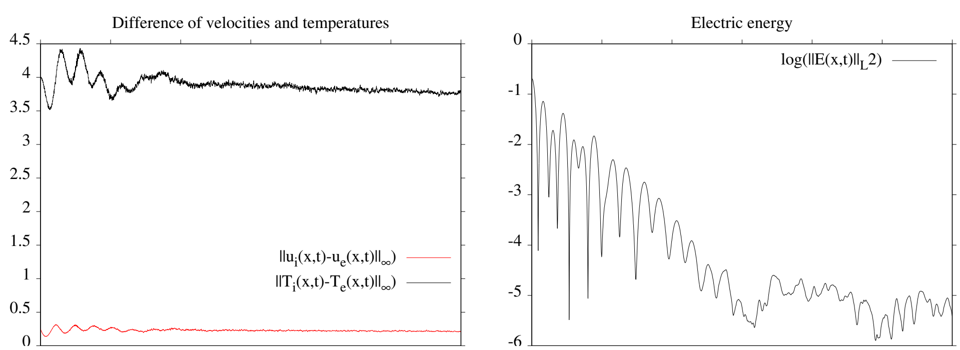

FIG. 10. *General case, $\alpha = 0.1$, $\varepsilon_i = \varepsilon_e = \tilde{\varepsilon_i} = \tilde{\varepsilon_e} = 1000$. Evolution in time of $||u_i(x, t) - u_e(x, t)||_\infty$ and $||T_i(x, t) - T_e(x, t)||_\infty$ (left), and of $\mathcal{E}(t)$ (right).*

Even at time $T = 60$, the velocities (resp. temperatures) of electrons and ions are very different. There is no global equilibrium.

Otherwise, these figures show that the results are affected by some numerical noise. This is a classical effect of particle methods, due to the probabilistic character of the initialisation. This noise affects macroscopic quantities because of the coupling between micro and macro equations. At fixed parameters (α, collision frequencies, N_x, *etc.*), the noise can be reduced by increasing the number of particles. In fact, the noise means that we have not enough particles per cell to represent the distribution function (g_{ee} or g_{ii} here). But thanks to the micro-macro decomposition, we only represent the perturbations g_{ee} and g_{ii} with particles, and not the whole functions f_e and f_i. So when g_{ee} (resp. g_{ii}) becomes smaller, fewer particles are necessary. It means that if f_e (resp. f_i) goes towards its equilibrium M_e (resp. M_i), the required number of particles diminishes. This is the main reason for using a micro-macro scheme with a particle method for the micro part.

The second testcase consists in an intermediate regime with $\varepsilon_i = \varepsilon_e = \tilde{\varepsilon_i} = \tilde{\varepsilon_e} = 1$. Collisions are enough frequent to bring the system towards a global equilibrium, as we can see on figure 11 at time $T = 0.5$ and then on figure 12 at time $T = 6$.

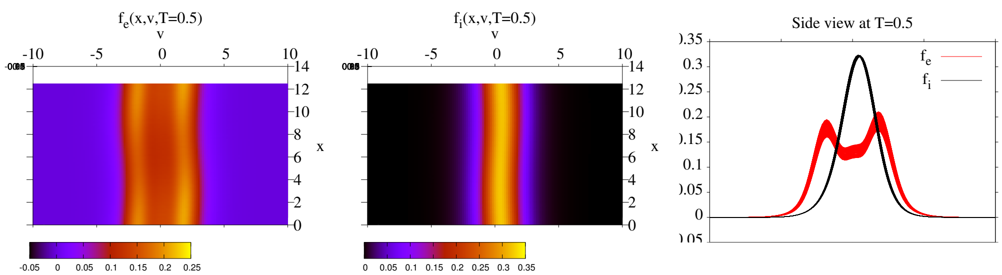

FIG. 11. *General case,* $\alpha = 0.1$*,* $\varepsilon_i = \varepsilon_e = \tilde{\varepsilon_i} = \tilde{\varepsilon_e} = 1$*. Distribution functions at time* $T = 0.5$*:* $f_e(x, v, T)$ *in phase-space (left),* $f_i(x, v, T)$ *in phase-space (middle), side view of* $f_e(x, v, T)$ *and* $f_i(x, v, T)$ *(right).*

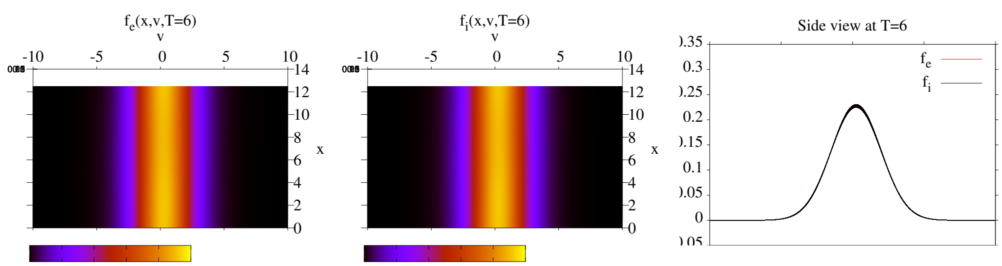

FIG. 12. *General case,* $\alpha = 0.1$*,* $\varepsilon_i = \varepsilon_e = \tilde{\varepsilon_i} = \tilde{\varepsilon_e} = 1$*. Distribution functions at time* $T = 6$*:* $f_e(x, v, T)$ *in phase-space (left),* $f_i(x, v, T)$ *in phase-space (middle), side view of* $f_e(x, v, T)$ *and* $f_i(x, v, T)$ *(right).*

The evolution in time of $||u_i(x, t) - u_e(x, t)||_\infty$ and $||T_i(x, t) - T_e(x, t)||_\infty$, presented on figure 13 (left), confirms the convergence towards a global equilibrium. On figure 13 (right), the evolution in time of the electric energy $\mathcal{E}(t)$ is presented.

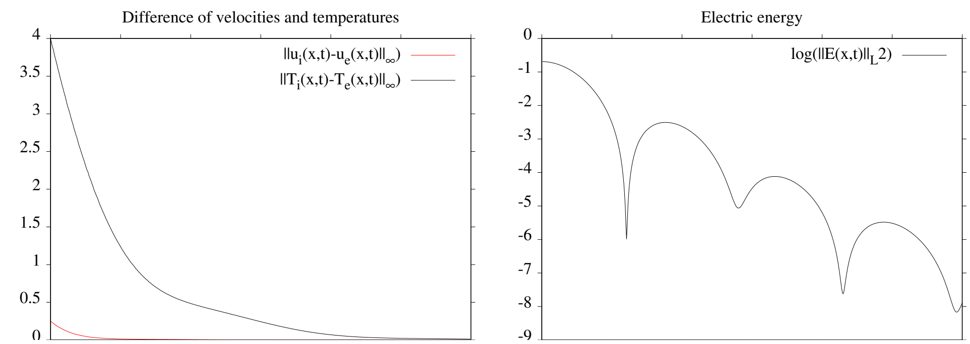

FIG. 13. *General case,* $\alpha = 0.1$*,* $\varepsilon_i = \varepsilon_e = \tilde{\varepsilon_i} = \tilde{\varepsilon_e} = 1$*. Evolution in time of* $||u_i(x,t) - u_e(x,t)||_\infty$ *and* $||T_i(x,t) - T_e(x,t)||_\infty$ *(left), and of* $\mathcal{E}(t)$ *(right).*

We expect that the convergence towards a global equilibrium is faster when collisions are more frequent. We will highlight this in the following test. For a convergence of the densities in short time, we now take $\alpha = 10^{-2}$ and $N_{p_e} = N_{p_i} = 5 \cdot 10^3$, $N_x = 128$ and $\Delta t = 10^{-3}$. Other parameters are unchanged and particularly we still have $n_e(x,0) = 1 + \alpha \cos(kx)$, $u_e(x,0) = 0$, $T_e(x,0) = 5\,(1 + \alpha \cos(kx))$, $n_i(x,0) = 1$, $u_i(x,0) = 1/2$ and $T_i(x,0) = 1$. For $\varepsilon_i = \varepsilon_e = \tilde{\varepsilon_i} = \tilde{\varepsilon_e} = 10^{-2}$, distribution functions are plotted on figure 14 at time $T = 0.01$ and then on figure 15 at time $T = 0.1$.

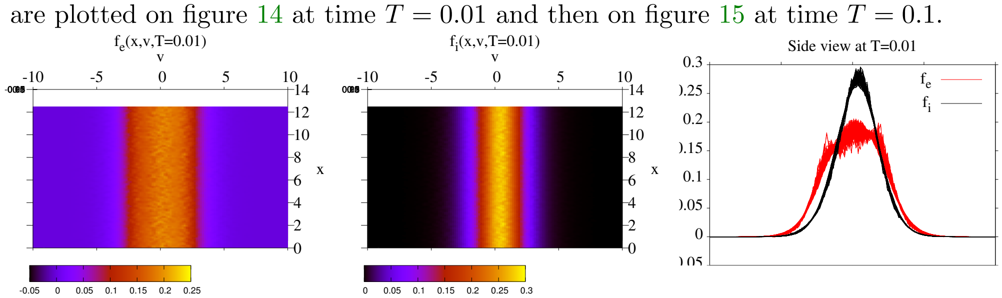

FIG. 14. *General case,* $\alpha = 10^{-2}$*,* $\varepsilon_i = \varepsilon_e = \tilde{\varepsilon_i} = \tilde{\varepsilon_e} = 10^{-2}$*. Distribution functions at time* $T = 0.01$*:* $f_e(x,v,T)$ *in phase-space (left),* $f_i(x,v,T)$ *in phase-space (middle), side view of* $f_e(x,v,T)$ *and* $f_i(x,v,T)$ *(right).*

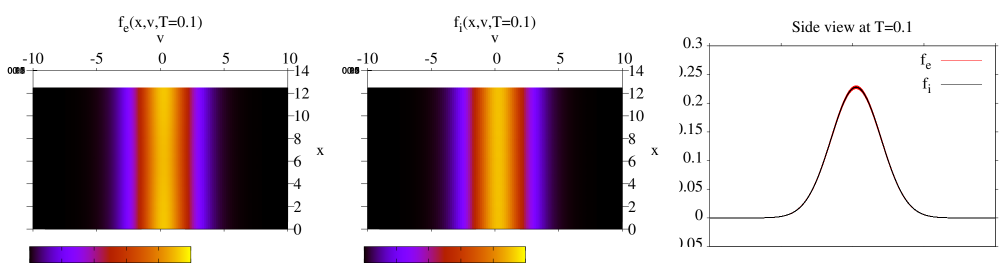

FIG. 15. *General case,* $\alpha = 10^{-2}$*,* $\varepsilon_i = \varepsilon_e = \tilde{\varepsilon_i} = \tilde{\varepsilon_e} = 10^{-2}$*. Distribution functions at time* $T = 0.1$*:* $f_e(x,v,T)$ *in phase-space (left),* $f_i(x,v,T)$ *in phase-space (middle), side view of* $f_e(x,v,T)$ *and* $f_i(x,v,T)$ *(right).*

We can see that the distribution functions are very close from each other at $T = 0.1$. The evolution in time of $||u_i(x,t) - u_e(x,t)||_\infty$ and $||T_i(x,t) - T_e(x,t)||_\infty$, presented on figure 16 (left), confirms the convergence of velocities and temperatures. We can see the evolution of $\mathcal{E}(t)$ on figure 16 (right).

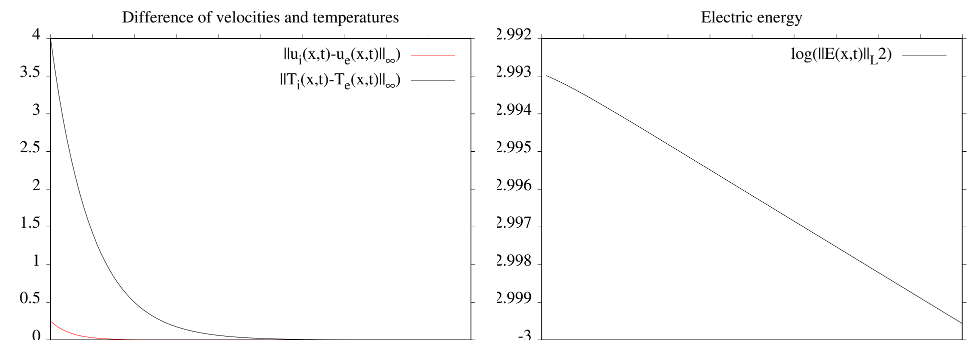

FIG. 16. *General case,* $\alpha = 10^{-2}$*,* $\varepsilon_i = \varepsilon_e = \tilde{\varepsilon_i} = \tilde{\varepsilon_e} = 10^{-2}$*. Evolution in time of* $||u_i(x,t) - u_e(x,t)||_\infty$ *and* $||T_i(x,t) - T_e(x,t)||_\infty$ *(left), and of* $\mathcal{E}(t)$ *(right).*

Finally, we propose a testcase in which the collisions between particles of the same species are frequent, whereas collisions between ions and electrons are infrequent. More precisely, we take $\alpha = 10^{-2}$, $N_{p_e} = N_{p_i} = 5 \cdot 10^3$, $N_x = 128$, $\Delta t = 10^{-2}$, $\varepsilon_i = \varepsilon_e = 10^{-2}$ and $\tilde{\varepsilon_i} = \tilde{\varepsilon_e} = 1000$. Distribution functions are presented on figure 17 at time $T = 0.01$ and then on figure 18 at time $T = 6$.

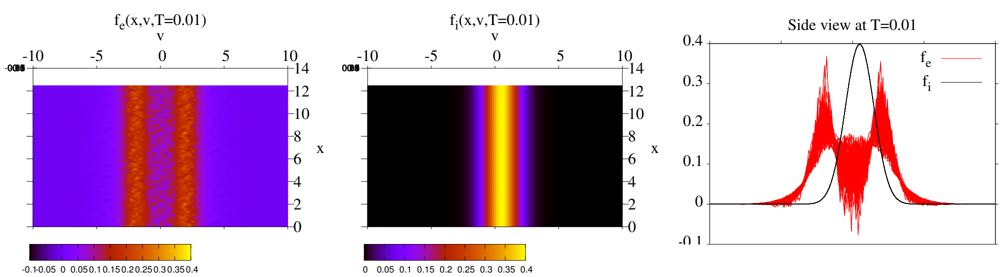

FIG. 17. *General case,* $\alpha = 10^{-2}$*,* $\varepsilon_i = \varepsilon_e = 10^{-2}$*,* $\tilde{\varepsilon_i} = \tilde{\varepsilon_e} = 1000$*. Distribution functions at time* $T = 0.01$*:* $f_e(x,v,T)$ *in phase-space (left),* $f_i(x,v,T)$ *in phase-space (middle), side view of* $f_e(x,v,T)$ *and* $f_i(x,v,T)$ *(right).*

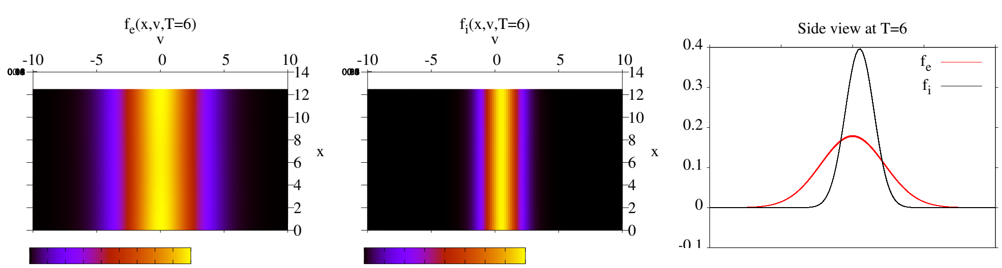

FIG. 18. *General case,* $\alpha = 10^{-2}$*,* $\varepsilon_i = \varepsilon_e = 10^{-2}$*,* $\tilde{\varepsilon_i} = \tilde{\varepsilon_e} = 1000$*. Distribution functions at time* $T = 6$*:* $f_e(x,v,T)$ *in phase-space (left),* $f_i(x,v,T)$ *in phase-space (middle), side view of* $f_e(x,v,T)$ *and* $f_i(x,v,T)$ *(right).*

Electrons tend to have a Maxwellian distribution function, but collisions between them and ions are to infrequent to bring the system to a global equilibrium, at least at time $T = 6$. The evolution of $||u_i(x,t) - u_e(x,t)||_\infty$ and $||T_i(x,t) - T_e(x,t)||_\infty$ is presented on figure 19 (left) and $\mathcal{E}(t)$ is presented on figure 19 (right).

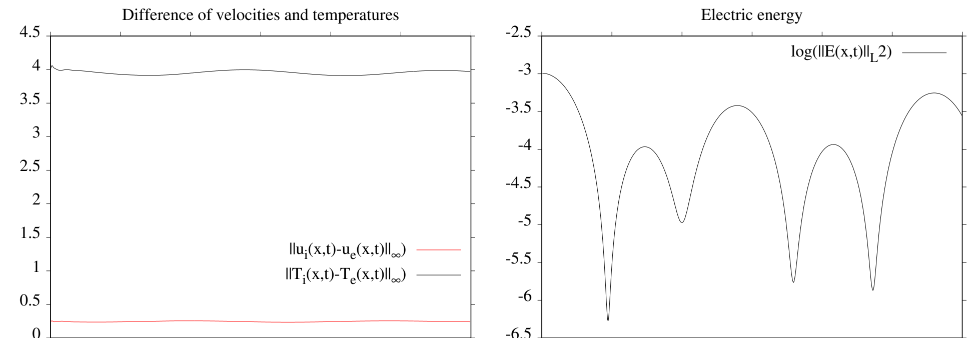

FIG. 19. *General case,* $\alpha = 10^{-2}$, $\varepsilon_i = \varepsilon_e = 10^{-2}$, $\tilde{\varepsilon_i} = \tilde{\varepsilon_e} = 1000$. *Evolution in time of* $||u_i(x,t) - u_e(x,t)||_\infty$ *and* $||T_i(x,t) - T_e(x,t)||_\infty$ *(left), and of* $\mathcal{E}(t)$ *(right).*

The numerical noise that we see on figure 17 means that there is not enough particles initially to represent in a good way g_{ee}. Indeed, this quantity is big at $T = 0$ since f_e is far from an equilibrium. But f_e goes fast towards a Maxwellian, so that g_{ee} becomes small and $N_{p_e} = 5 \times 10^3$ particles is then sufficient. This explains why this noise is no longer perceptible as time goes by.

Let us remark that in a full particle method on f_e and f_i (in a model without micro-macro decomposition), many more particles are necessary, since the distribution functions f_e and f_i keep the same order of magnitude as time goes by. So the cost of a full particle method is constant with respect to the collision frequencies. On the contrary, the cost of our micro-macro model is reduced when ε_e and ε_i decrease.

7. Conclusion. In this paper, we first present a new model for a two species 1D Vlasov-BGK system based on a micro-macro decomposition. This one, derived from [17], separates the intra and interspecies collision frequencies. Thus, the convergence of the system towards a global equilibrium can, depending on the values of the collision frequencies, be separated into two steps: the convergence towards the own equilibrium of each species and then towards the global one. Moreover, in the space-homogeneous case without electric field, we estimate the convergence rate of the distribution functions towards the equilibrium, as well as the convergence rate of the velocities (resp. temperatures) towards the same value.

Then, we derive a scheme using a particle method for the kinetic micro part and a standard finite volume method for the fluid macro part. In the space-homogeneous case, we illustrate numerically the convergence rates of velocities and temperatures and verify that it is in accordance with the estimations. Finally, in the general case, we propose testcases to see the evolution in time of the distribution functions and their convergence towards equilibrium. The main advantage of this particle micro-macro approach is the reduction of the numerical cost, especially in the fuid limit, where few particles are sufficient.

Acknowledgments. The authors would like to thanks Eric Sonnendrücker for useful discussions and suggestions about this paper.

This work has been supported by the PHC Procope DAAD Program and by the SCIAS Fellowship Program. Moreover, Anaïs Crestetto is supported by the French ANR project ACHYLLES ANR-14-CE25-0001 and Marlies Pirner is supported by the German Priority Program 1648.

REFERENCES

[1] P. Andries, K. Aoki, and B. Perthame, A consistent bgk-type model for gas mixtures, Journal of Statistical Physics, 106 (2002), pp. 993–1018, https://doi.org/10.1023/A:1014033703134, http://dx.doi.org/10.1023/A:1014033703134.

[2] P. M. Bellan, Fundamentals of Plasma Physics, Cambridge University Press, 2008.

[3] M. Bennoune, M. Lemou, and L. Mieussens, Uniformly stable numerical schemes for the boltzmann equation preserving the compressible navierstokes asymptotics, Journal of Computational Physics, 227 (2008), pp. 3781 – 3803, https://doi.org/http://dx.doi.org/10.1016/j.jcp.2007.11.032, http://www.sciencedirect.com/science/article/pii/S0021999107005268.

[4] F. Bernard, A. Iollo, and G. Puppo, Accurate asymptotic preserving boundary conditions for kinetic equations on cartesian grids, Journal of Scientific Computing, 65 (2015), pp. 735–766, https://doi.org/10.1007/s10915-015-9984-8, http://dx.doi.org/10.1007/s10915-015-9984-8.

[5] C. Besse, P. Degond, F. Deluzet, J. Claudel, G. Gallice, and C. Tessieras, A model hierarchy for ionospheric plasma modeling., Math. Models Meth. Appl. Sci., 14 (2004), pp. 393–415, https://hal.archives-ouvertes.fr/hal-00018457.

[6] C. Birdsall and A. Langdon, Plasma Physics via Computer Simulation, Series in Plasma Physics and Fluid Dynamics, Taylor & Francis, 2004, https://books.google.de/books?id=S2lqgDTm6a4C.

[7] A. Crestetto, N. Crouseilles, and M. Lemou, Kinetic/fluid micro-macro numerical schemes for Vlasov-Poisson-BGK equation using particles, Kinetic and Related Models , 5 (2012), pp. 787–816, https://doi.org/10.3934/krm.2012.5.787, https://hal.inria.fr/hal-00728875.

[8] N. Crouseilles and M. Lemou, An asymptotic preserving scheme based on a micro-macro decomposition for collisional vlasov equations: diffusion and high-field scaling limits, Kinetic and Related Models, 4 (2011), pp. 441–477, https://doi.org/10.3934/krm.2011.4.441, http://aimsciences.org/journals/displayArticlesnew.jsp?paperID=6088.

[9] A. De Cecco, F. Deluzet, C. Negulescu, and S. Possanner, Asymptotic transition from kinetic to adiabatic electrons along magnetic field lines, Multiscale Model. Simul., 15 (2017), p. 309338, https://doi.org/10.1137/15M1043686.

[10] P. Degond and G. Dimarco, Fluid simulations with localized boltzmann upscaling by direct simulation monte-carlo, Journal of Computational Physics, 231 (2012), pp. 2414 – 2437, https://doi.org/http://dx.doi.org/10.1016/j.jcp.2011.11.030, http://www.sciencedirect.com/science/article/pii/S0021999111006851.

[11] G. Dimarco, L. Mieussens, and V. Rispoli, An asymptotic preserving automatic domain decomposition method for the vlasovpoissonbgk system with applications to plasmas, Journal of Computational Physics, 274 (2014), pp. 122 – 139, https://doi.org/http://dx.doi.org/10.1016/j.jcp.2014.06.002, http://www.sciencedirect.com/science/article/pii/S0021999114004069.

[12] G. Dimarco and L. Pareschi, Numerical methods for kinetic equations, Acta Numerica, (2014), pp. 369–520, https://hal.archives-ouvertes.fr/hal-00986714.

[13] F. Filbet and S. Jin, A class of asymptotic-preserving schemes for kinetic equations and related problems with stiff sources, Journal of Computational Physics, 229 (2010), pp. 7625 – 7648, https://doi.org/http://dx.doi.org/10.1016/j.jcp.2010.06.017, http://www.sciencedirect.com/science/article/pii/S0021999110003323.

[14] E. P. Gross and M. Krook, Model for collision processes in gases: Small-amplitude oscillations of charged two-component systems, Phys. Rev., 102 (1956), pp. 593–604, https://doi.org/10.1103/PhysRev.102.593, https://link.aps.org/doi/10.1103/PhysRev.102.593.

[15] B. B. Hamel, Kinetic model for binary gas mixtures, Physics of Fluids, 8 (1965), pp. 418–425, https://doi.org/10.1063/1.1761239, http://aip.scitation.org/doi/abs/10.1063/1.1761239, https://arxiv.org/abs/http://aip.scitation.org/doi/pdf/10.1063/1.1761239.

[16] S. Jin and Y. Shi, A micro-macro decomposition-based asymptotic-preserving scheme for the multispecies boltzmann equation, SIAM Journal on Scientific Computing, 31 (2010), pp. 4580–4606, https://doi.org/10.1137/090756077, https://doi.org/10.1137/090756077, https://arxiv.org/abs/https://doi.org/10.1137/090756077.

[17] C. Klingenberg, M. Pirner, and G. Puppo, A consistent kinetic model for a two-component mixture with an application to plasma, Kinetic and Related Models, 10 (2017), pp. 445–465, https://doi.org/10.3934/krm.2017017, http://aimsciences.org/journals/displayArticlesnew.jsp?paperID=13371.

[18] D. Matthes, Lecture notes on the course entropy methods and related functional”.

[19] S. Pieraccini and G. Puppo, Implicit–explicit schemes for bgk kinetic equations, Journal of Scientific Computing, 32 (2007), pp. 1–28, https://doi.org/10.1007/s10915-006-9116-6, http://dx.doi.org/10.1007/s10915-006-9116-6.
[20] L. Saint-Raymond, Hydrodynamic Limits of the Boltzmann Equation, no. nr. 1971 in Hydrodynamic Limits of the Boltzmann Equation, Springer, 2009, https://books.google.nl/books?id=ROUILXXb7UUC.